We thank the reviewers for their thoughtful feedback, which has helped us to further improve and strengthen the manuscript. Our detailed responses to the final reviewer comments are provided below in blue. All revisions are visible in the track-changes version of the revised manuscript and shown below in green.

We note that, during the review process, we conducted an intercomparison between the original PUFIN system, a newly built duplicate unit, and our standard ARM ground-based INP filters as presented in Creamean et al. (2025). All filters were collected outside our building at CSU for 30 minutes. We added a figure showing the resulting spectra in the Supporting Information and included text describing this intercomparison in Section 4.3: Two identical PUFIN units are currently available, including the original system and a newly constructed duplicate. An intercomparison test was conducted using standard ARM ground-based INP filters (Creamean et al., 2025), in which ambient samples were collected outside CSU for 30 minutes, using the first sample valves on both PUFIN systems. The resulting INP spectra show good agreement between the two units, and the ground-based INP filters deployed routinely at ARM sites, demonstrating reproducibility and consistency in sampling and analysis (see Figure S5).

RC1

The manuscript presents a newly developed payload, "PUFIN," for vertically resolved sampling of ice-nucleating particles (INPs) using tethered balloon systems. The PUFIN system samples aerosol particles with a powerful scroll pump onto polycarbonate filters in three separate filter holders, each selected for sampling at a different altitude, using remote-controlled magnetic valves. INP abundance and temperature spectra are derived from offline filter analysis using an INP detection system (here, the Colorado State University INS). This is a very valuable approach to extending INP sampling into the vertical with tethered balloon systems, particularly because multiple filters allow contrasting altitudes, such as the free troposphere from the boundary layer. The paper is very well written and provides a sound description of the PUFIN system, its deployments across the US, and the INP analysis of the sampled filters. The INP community may also benefit from the author's open-source approach, which provides technical drawings and details about PUFIN in a public repository, as well as freely available INP data from their previous balloon deployments. I recommend accepting the manuscript for publication in AMT.

We thank the reviewer for their overall assessment and appreciate their perspective on how this work will benefit the INP community!

Some recommendations for improvements are listed below:

1. The manuscript could benefit from showing meteorological data from the iMet-XQ2, particularly given that the INP samples exhibit varying abundance at different altitudes, rather than simply assuming atmospheric layering as the sole explanation (e.g., lines 303-305, 320). This could further emphasize the need for vertically resolved INP sampling.

This is a good point. Unfortunately, for the February flights, the iMet-XQ2 data were not recorded in the INP flight data files, although they are available for the July flights. In addition, the accuracy of the iMet-XQ2 measurements is limited (see below), so we instead use the more reliable "TBSIMET" data to examine

equivalent potential temperature, calculated following Bolton (1980). This parameter is well suited for assessing atmospheric stratification and boundary layer mixing.

We added two new figures to the Supporting Information and included the following text at the beginning of Section 4.2: We also evaluated equivalent potential temperature (θ_e) during flight days using data collected from the TBS to assess whether the boundary layer in the PUFIN sampling region was well mixed, where INP concentrations would be expected to be similar across altitudes, or stratified, which can promote aerosol layering (Creamean et al., 2021; Griesche et al., 2021, 2025). Details of the θ_e calculations are provided in the Supporting Information.

Throughout Section 4.2, we added supporting evidence showing that, on days with two spectra that differed significantly, these differences were often associated with a stratified boundary layer based on θ_e profiles. Please refer to the tracked changes version of the manuscript below to see where these additions were made, as they are distributed throughout the section.

In the Supporting Information, we added the following methods:

Because the iMet-XQ2 accuracy is limited (see Summary section), we use the more reliable TBSIMET observations to examine equivalent potential temperature (θe), calculated following Bolton (1980), which is well suited for assessing atmospheric stratification and boundary-layer mixing. Additionally, for the CRG February flights the iMet-XQ2 data were not recorded in the INP flight data files, although iMet-XQ2 measurements were taken for the July flights. TBSIMET data are available from the ARM Data Center (https://adc.arm.gov/discovery/results/s::tbsimet).

To calculate θe, TBSIMET data (altitude, temperature, pressure, relative humidity) were first preprocessed by removing unrealistic, non-NaN spikes in altitude observations and converting altitude from kilometers to meters. The profiles were then averaged into 10-m vertical bins; within each bin the mean altitude, temperature (°C), pressure (hPa), and relative humidity (%) were computed. Dew point temperature (T_d) in each bin was estimated from the binned temperature and relative humidity using the Magnus–Tetens approximation. Saturation vapor pressure at T_d was computed and the mixing ratio r (kg kg^{-1}) obtained via $r = \varepsilon e_s/(p - e_s)$ with $\varepsilon = 0.622$. Potential temperature θ was calculated from the binned temperature and pressure, and equivalent potential temperature was computed using the Bolton (1980) formulation: $\theta e = \theta \exp((L_v r)/(c_p T_d(K)))$, where L_v is latent heat of vaporization ($\approx 2.5\times10^6$ J kg^{-1}), c_p is the dry-air specific heat at constant pressure (≈ 1005.7 J kg^{-1} K^{-1}), and $T_d(K)$ is T_d in kelvin. Uncertainty in θ_e was estimated as the one-standard-deviation of θ_e values computed for each original sample within a bin (i.e., compute θ_e per sample, then take the binwise standard deviation).

To determine whether the boundary layer at the PUFIN sampling altitudes was well mixed or stratified, we evaluated θ_e only within the altitude ranges where PUFIN was deployed. If the vertical variation (minimum to maximum) in θ_e was ≤ 1 K, the layer was considered well mixed; if > 1 K, it was classified as stratified. Variability in θ_e could manifest as discrete layers or as a continuous vertical gradient.

Bolton, D.: The Computation of Equivalent Potential Temperature, Mon. Wea. Rev., 108, 1046–1053, https://doi.org/10.1175/1520-0493(1980)108%3C1046:TCOEPT%3E2.0.CO;2, 1980.

Griesche, H. J., Engelmann, R., Radenz, M., Hofer, J., Althausen, D., Ansmann, A., Barry, K., Creamean, J., Jimenez, C., and Seifert, P.: Annual cycle of surface-coupling effects on Arctic mixed-phase clouds during MOSAiC, EGUsphere, 1–33, https://doi.org/10.5194/egusphere-2025-5708, 2025.

2. Some more background on the sampling strategy would be nice. For instance, why were the specific sampling altitudes chosen? Which atmospheric layers are of interest?

PUFIN sampling is conducted concurrently with other airborne measurements that provide particle size distributions and multimodal micro-spectroscopy, yielding single-particle and molecular-level information on atmospheric aerosols at different altitudes. These complementary measurements predate PUFIN deployment on the ARM TBS and are typically performed within predefined altitude ranges to facilitate comparisons across flight days, seasons, and locations. Although altitude bins are adjusted based on flight conditions and available time, they are generally targeted at ~0–250 m, 250–500 m, and >500 m AGL. As shown in Figures 5 and 6, these ranges were not always strictly followed during the initial PUFIN flights due to operational constraints. Along these lines, we updated the figure legends to reflect the correct start and end altitudes based on TBSIMET data, which are more accurate and available through the ARM Data Center (Dexheimer et al., 2024).

We added new text on sampling strategy in Section 2.4.2: PUFIN sampling is often conducted in coordination with concurrent airborne measurements, including aerosol size distributions and multimodal micro-spectroscopy, to enable complementary characterization of aerosol properties across altitudes. Sampling is performed within predefined altitude ranges to facilitate comparison across flights, seasons, and locations, targeting roughly 0–250 m, 250–500 m, and >500 m AGL. These altitude bins are adjusted as needed based on flight duration and atmospheric conditions. They can be modified in real time to target layers of interest identified from on-site aerosol and meteorological measurements.

We also added the following to Section 2.2: However, these measurements are only accurate to approximately ±20 m; therefore, altitude data are taken from the TBS iMet system, available as the "TBSIMET" datastream from the ARM Data Center (Dexheimer et al., 2024).

3. Is it possible to derive a recommendation for the minimum sampling time in differing environments or seasons from the provided results in Section 4.2? A brief "lessons-learned" could also foster PUFIN rebuilds and deployments by other groups.

This is an excellent question. While we would like to provide recommendations for minimum sampling times, we are still building the necessary experience to reliably and robustly do so. To date, PUFIN measurements have been conducted at only two sites (CRG and BNF). Although additional sites have been sampled using IcePuck (with the combined deployments spanning urban, forest, agricultural, and mountain environments) these differed in terms of flow rates, sampling altitudes, and seasons, limiting our ability to draw generalized conclusions. We anticipate that, as we expand observations across a broader range of sites and conditions, we will be better positioned to offer such recommendations in the future.

That said, we agree that including a brief "lessons learned" discussion is a valuable suggestion, and we now added the following text to the Summary section: As PUFIN has only been deployed a limited number of

times to date, we are still actively identifying best practices. While we have not yet fully evaluated performance under extreme environmental conditions, future deployments will require careful consideration of such factors. Initial experience highlights the importance of maximizing sampling volume for robust INP detection and the value of sending test samples from new or unfamiliar environments for immediate analysis to inform subsequent sampling strategies. We also note that inlet components (e.g., hose barbs) may introduce minor collection efficiency losses, though further testing is needed to assess potential trade-offs with background contamination during ascent and descent. Maintaining consistent altitude ranges where possible improves comparability, and future dedicated flights are planned to include longer-duration sampling at fixed "loitering" altitudes to better resolve vertical structure and potentially achieve even lower detection limits.

4. Figure 5 is difficult to interpret due to overlapping dots. Is each data point shown, or could one point be entirely covered by another? A separation into seasons might be helpful, as the temperature spectra are not only sampling time-dependent.

Figure 5 generated confusion among both reviewers and did not substantially contribute to the overall narrative. It was only briefly described in the text and was not essential for conveying the main points. Therefore, we chose to remove the figure to improve clarity.

5. Some more interpretation and discussion of the derived temperature spectra in section 4.2 would be interesting, e.g., line 309: Which INP types are representative of the winter spectra?

We appreciate the reviewer's interest in further interpretation of the derived temperature spectra and agree that exploring which INP types are represented would be scientifically valuable. However, a detailed analysis and interpretation of these features falls beyond the primary scope of this manuscript and the focus of *Atmospheric Measurement Techniques*, which emphasizes instrumentation, methods, and data availability. Our intent in Section 4.2 was to provide an initial presentation of the temperature spectra to demonstrate the capabilities of the dataset and to highlight its potential for future scientific investigation. In this sense, the spectra are meant to serve as a preview that encourages the community to further explore these data in combination with complementary meteorological and aerosol measurements. A more in-depth discussion of the underlying processes and attribution to specific INP types would be better suited for a study centered on scientific interpretation, such as one aligned with the scope of a journal like *Atmospheric Chemistry and Physics*.

We chose not to expand substantially on the interpretation in order to maintain focus and coherence with the goals of the paper. We clarified this intent by adding the following at the beginning of Section 4.2: The objective of this section is to provide an initial presentation of the temperature spectra, demonstrating the capabilities of the dataset and highlighting its potential for future scientific investigation. A more in-depth scientific interpretation of these data falls beyond the primary scope of this manuscript; however, we encourage the community to further explore these observations in combination with complementary meteorological and aerosol measurements.

RC2

General:

Creamean et al., 2025, describes the development of an aerosols sampling system (PUFIN) with focus on deployment on tethered balloon systems. The authors successfully built a system capable of sampling ice nucleating particles (INPs) in vertical profiles. Ice nucleation measurements were conducted downstream after extracting INPs from the filters of PUFIN. The technology is of great value for the scientific community, and the paper is very well suited for publication in AMT. Especially the accessibility to the data and possibility to request PUFIN for field measurements is highly appreciated. Nevertheless, the paper could be significantly improved by comparing the results and the sampling technique with literature and explain the example dataset in more detail. A discussion of the advantages and disadvantages of the sampling technique in comparison with other UAS and balloon systems and sampling techniques (e.g. impinger or impactor) could further improve the study. Therefore, I suggest the publication of the study after minor revisions.

We thank the reviewer for recognizing the accessibility of the dataset and for highlighting these shortcomings in our manuscript.

Key Considerations:

Introduction

The introduction is well written and summarizes important knowledge and state of the art about aerosol and INP measurement at different heights in the troposphere. The authors also discuss the advantages of tethered balloon systems (TBS) over uncrewed aerial systems (UAS), such as longer sampling times. However, I was wondering how the flight path and position of sampling is different between TBS and UAS. For example, using fixed-wing drones[1] or rotary wing drones[2–4] could allow for a more precise flight path and location than a balloon system which also relies on the wind conditions and ground accessibility of the sampling locations. Furthermore, I was wondering what the key advantages of the PUFIN system are over the SHARK kit.[5] I wish the authors could address the key differences in the introduction or in the discussion of the paper. A table comparing different unoccupied sampling tools for INPs[3,5,6] could be helpful in understanding the need for PUFIN.

While UAS platforms indeed can offer more precise control over flight paths and sampling locations, they are often constrained by shorter flight durations, payload limitations, and regulatory restrictions. In contrast, TBS deployments can operate for extended periods (up to ~6–8 hours), enabling longer sampling times and sufficient particle collection at multiple altitude levels (up to three) within a single flight. This extended sampling capability is particularly advantageous for INP measurements, where sufficient loading is critical.

We expanded Section 4.2 to include a comparison of INP concentrations from recent balloon-borne and UAS-based studies: At −20 °C, the INP concentrations observed at CRG (0.01–1 L^{-1} in winter; 0.01–12 L^{-1} in summer) and BNF (0.01–1 L^{-1} in spring; 0.02–11 L^{-1} in summer) fall within the broad range reported in recent studies. For example, Creamean et al. (2018) reported 1–11 L^{-1} in springtime agricultural regions in Colorado from vertically-resolved filters via a launched and retrieved balloon system, while similar concentrations (~0.02–12 L^{-1}) were observed by Bieber et al. (2020) and Seifried et al. (2021) near a lake in Austria in summer via UAS. Böhmländer et al. (2025) reported lower values of ~0.2–0.5 L^{-1} during

spring and autumn UAS test flights in a boreal environment in Finland. In April in Cyprus, Marinou et al. (2019) reported ~3 L^{-1} from UAS measurements. Values ranging from ~0.2–10 L^{-1} from size-resolved measurements have been reported by Porter et al. (2020) across multiple sites in Europe and the Arctic using balloon-based sampling. Overall, the concentrations reported here are consistent with the range of environments sampled in the literature, spanning relatively clean to more biologically or terrestrially influenced regions.

As noted in the introduction, previous work such as Porter et al. (2020) and Böhmländer et al. (2025) highlights the strengths of alternative approaches. We agree that instruments such as SHARK provide valuable measurements, but all techniques, including PUFIN, have inherent limitations. While SHARK offers important size-resolved information, it is currently limited to sampling at a single altitude. However, these methods and PUFIN are complementary rather than competing. One key aspect that distinguishes PUFIN is that, unlike existing systems typically developed within individual PI-led efforts, PUFIN is designed for deployment within the ARM user facility to provide accessible, community-driven measurements. Users can request the PUFIN systems for deployments and access data without the need to build or operate specialized instrumentation or process the samples via drop freezing assays themselves.

In response to the reviewer's suggestion, we also broadened the discussion to include additional relevant studies in the Introduction to better contextualize PUFIN within the existing literature: Bieber et al. (2020) and Seifried et al. (2021) describe a developed system, the DAPSI (Drone-based Aerosol Particle Sampling Impinger/Impactor), for collecting INP samples using UAS. To date, results have been limited to test flights and a short (3-day) campaign conducted near a lake in Austria during summer.

Bieber, P., Seifried, T. M., Burkart, J., Gratzl, J., Kasper-Giebl, A., Schmale, D. G., and Grothe, H.: A Drone-Based Bioaerosol Sampling System to Monitor Ice Nucleation Particles in the Lower Atmosphere, Remote Sensing, 12, 552, https://doi.org/10.3390/rs12030552, 2020.

Seifried, T. M., Bieber, P., Kunert, A. T., Iii, D. G. S., Whitmore, K., Fröhlich-Nowoisky, J., and Grothe, H.: Ice Nucleation Activity of Alpine Bioaerosol Emitted in Vicinity of a Birch Forest, Atmosphere, 12, https://doi.org/10.3390/atmos12060779, 2021.

Methods

PUFIN samples INPs on filters which can be further extracted for ice nucleation experiments. Their workflow is clever and straightforward, the cleaning procedures and the immediate cooling of the samples to -80°C prior INP measurements with the CSU INS is thorough. However, there are some remaining questions which I think deserve attention prior publication: What is the size cutoff and sampling efficiency for aerosol sampling on the filter? How do the authors make sure that all INPs are washed of the filter? What is the advantage of sampling INPs on filters over impingers[7] or impactors[5]? Does the developed sampling procedure limit downstream analysis of INPs, for example cultivation of ice nucleating microbes[7]? What is the total weight of the setup? Could it in theory also be applied for other balloons or UAS?

Based on the calculations of Spurny and Lodge (1972), the collection efficiencies of the 0.2-µm filters across the flow rate range at which PUFIN has operated at CRG and BNF (4-11 L min^{-1}) are relatively high.

As shown in the plots below, the sampling efficiency decreases around 150 nm, reaching minimum values of approximately 78–91%.

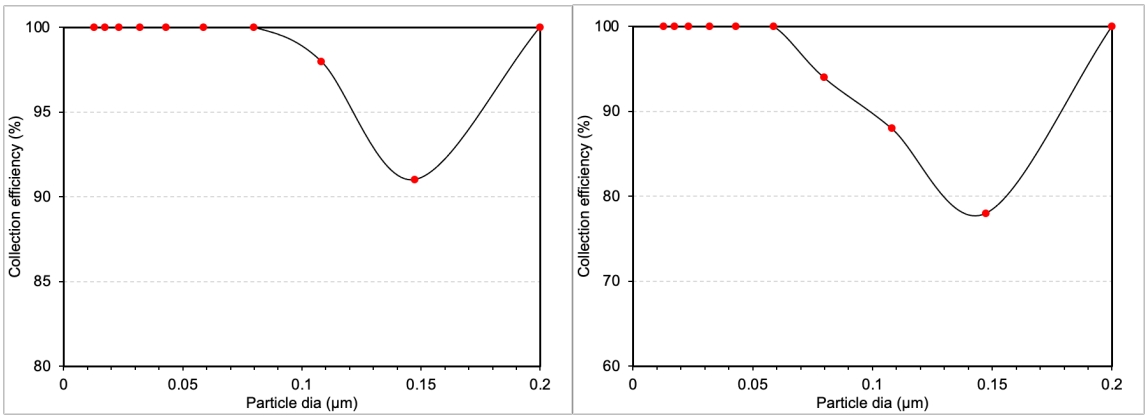

Collection efficiency plots at (left) 4 L min^{-1} and (right) 11 L min^{-1}.

In principle, these filters sample total suspended particulates (TSP); however, the use of in-line filter units introduces potential inlet-related biases, particularly for the largest particles. The transmission of larger particles into the inlet is likely influenced by wind speed and associated inertial and gravitational effects, which can reduce sampling efficiency for coarse-mode aerosols. From a particle transport perspective, such behavior would be governed by size-dependent losses characterized by parameters such as the Stokes number and settling velocity, suggesting that very large particles may be underrepresented. That said, these effects have not yet been empirically constrained for this system and remain an area for future characterization.

Regarding the removal method, in the past we tested rotation versus vortexing for the same extraction duration. Although vortexing is more aggressive in removing particles, it did not produce different results compared to rotation. Additionally, this technique has also been intercompared with other methods employing different particle removal approaches and shows good agreement (DeMott et al., 2017, 2025; Lasher et al., 2024). However, future work should explore a range of rotation times to confirm that 20 minutes is sufficient across filters with varying particle loadings. We added the following to the Summary section: For particle removal from the filters, this approach has been intercompared with other techniques employing different extraction methods and showed good agreement (DeMott et al., 2017, 2025; Lasher et al., 2024). Future work will evaluate a range of rotation times to ensure that the current 20-minute extraction is sufficient across filters with varying particle loadings.

Filters offer several advantages over impingers, particularly in terms of simplicity and robustness. They do not require liquid handling during sampling, are less sensitive to environmental conditions (e.g., temperature, humidity), and are easier to deploy in remote or harsh environments. In addition, impinger samples generally need to be analyzed more quickly, as INPs can evolve during storage in aqueous media, even when frozen, whereas INPs collected on filters tend to be more stable when stored frozen (e.g., Beall et al., 2020). Compared to impactors, filters provide a bulk-integrated sample rather than size-segregated fractions, which is advantageous when the goal is to quantify total INP concentrations across all particle sizes. Although this comes at the expense of size resolution, it simplifies analysis and reduces uncertainties

associated with particle bounce, re-entrainment, and stage-specific collection efficiencies. That said, each method has its strengths: impingers can better preserve particle hydration state and collect semi-volatile material, while impactors provide size-resolved information. Ultimately, the choice depends on the scientific objective. In general, filters offer a versatile, robust, and widely adopted approach for INP sampling, facilitating greater intercomparability across studies.

Downstream microbial analyses may be possible, but are unlikely with the sampling volumes and flow rates currently used, which limit the amount of biomass collected. Achieving sufficient loading for such analyses would require higher-flow systems like impingers or SASS samplers (https://www.resrchintl.com/products/sass-3100.php) operating at several hundred liters per minute, particularly over the relatively short sampling durations employed here. The primary objective of PUFIN is to obtain INP-resolved measurements at up to three altitudes within a single flight, which constrains available sampling time and precludes the longer durations that would be needed to accumulate adequate biomass. Extending flight times to meet these requirements would be operationally impractical. That said, this is a compelling direction. We are exploring opportunities with ARM users to incorporate miniaturized bioaerosol sampling alongside PUFIN in upcoming campaigns, including the DUSTIEAIM (https://armgov.svcs.arm.gov/research/campaigns/amf2026dustieaim) study in the coming year.

The total weight of PUFIN is 6.1 kg as stated on line 134.

To address your final question, the PUFIN systems are currently configured for deployment on the ARM TBS. However, in principle, the setups are flexible and could be adapted for use on other balloon platforms or UASs. If there is interest from the user community, we would welcome the opportunity to explore expanding PUFIN beyond its current platform. We added the following text to Section 4.3, which we also changed the title to "Requesting PUFIN for future ARM TBS campaigns and beyond": PUFIN is currently configured for deployment on the ARM user facility TBS system, but the design is flexible and could be adapted for use on other balloon platforms or UASs, contingent on community interest.

To address these, we now changed the title of section 2.4.1 to "Filter material and holder preparation" and added the following paragraph: The 0.2-µm filters used in PUFIN provide a simple, robust, and widely adopted approach for INP sampling, enabling bulk-integrated collection across particle sizes and facilitating intercomparability across studies. Compared to impingers, filters do not require liquid handling, are less sensitive to environmental conditions, and allow for more stable storage of INPs when frozen (e.g., Beall et al., 2020). Compared to impactors, they provide a bulk-integrated sample rather than size-segregated fractions, simplifying analysis and reducing uncertainties associated with particle bounce and stage-specific collection efficiencies. Based on calculations from Spurny and Lodge (1972), these filters exhibit relatively high collection efficiencies across PUFIN's operating flow rate range (4-11 L min^{-1}), with a decrease near 150 nm but still maintaining efficiencies on the order of 78–91%. In principle, the filters sample total suspended particulates. However, inlet-related biases, particularly for coarse particles, may arise due to wind speed-dependent inertial and gravitational losses (e.g., governed by Stokes number and settling velocity), such that the largest particles may be underrepresented, although this has not yet been empirically quantified for this system.

Beall, C. M., Lucero, D., Hill, T. C., DeMott, P. J., Stokes, M. D., and Prather, K. A.: Best practices for precipitation sample storage for offline studies of ice nucleation in marine and coastal environments, Atmos. Meas. Tech., 13, 6473–6486, https://doi.org/10.5194/amt-13-6473-2020, 2020.

DeMott, P. J., Hill, T. C. J., Petters, M. D., Bertram, A. K., Tobo, Y., Mason, R. H., Suski, K. J., McCluskey, C. S., Levin, E. J. T., Schill, G. P., Boose, Y., Rauker, A. M., Miller, A. J., Zaragoza, J., Rocci, K., Rothfuss, N. E., Taylor, H. P., Hader, J. D., Chou, C., Huffman, J. A., Pöschl, U., Prenni, A. J., and Kreidenweis, S. M.: Comparative measurements of ambient atmospheric concentrations of ice nucleating particles using multiple immersion freezing methods and a continuous flow diffusion chamber, Atmospheric Chem. Phys., 17, 11227–11245, https://doi.org/10.5194/acp-17-11227-2017, 2017.

DeMott, P. J., Mirrielees, J. A., Petters, S. S., Cziczo, D. J., Petters, M. D., Bingemer, H. G., Hill, T. C. J., Froyd, K., Garimella, S., Hallar, A. G., Levin, E. J. T., McCubbin, I. B., Perring, A. E., Rapp, C. N., Schiebel, T., Schrod, J., Suski, K. J., Weber, D., Wolf, M. J., Zawadowicz, M., Zenker, J., Möhler, O., and Brooks, S. D.: Field intercomparison of ice nucleation measurements: the Fifth International Workshop on Ice Nucleation Phase 3 (FIN-03), Atmospheric Measurement Techniques, 18, 639–672, https://doi.org/10.5194/amt-18-639-2025, 2025.

Lacher, L., Adams, M. P., Barry, K., Bertozzi, B., Bingemer, H., Boffo, C., Bras, Y., Büttner, N., Castarede, D., Cziczo, D. J., DeMott, P. J., Fösig, R., Goodell, M., Höhler, K., Hill, T. C. J., Jentzsch, C., Ladino, L. A., Levin, E. J. T., Mertes, S., Möhler, O., Moore, K. A., Murray, B. J., Nadolny, J., Pfeuffer, T., Picard, D., Ramírez-Romero, C., Ribeiro, M., Richter, S., Schrod, J., Sellegri, K., Stratmann, F., Swanson, B. E., Thomson, E. S., Wex, H., Wolf, M. J., and Freney, E.: The Puy de Dôme ICe Nucleation Intercomparison Campaign (PICNIC): comparison between online and offline methods in ambient air, Atmospheric Chem. Phys., 24, 2651–2678, https://doi.org/10.5194/acp-24-2651-2024, 2024.

Spurny, K. R. and Lodge, J. P.: Collection Efficiency Tables for Membrane Filters Used in the Sampling and Analysis of Aerosols and Hydrosols, Laboratory of Atmospheric Science, National Center for Atmospheric Research, 56 pp., 1972.

Results

Figure 5 could be discussed with more detail. What is the main message of this figure? That PUFIN has the advantage over IcePuck with the sampling time? This is not obvious to me as a reader.

Figure 5 generated confusion among both reviewers and did not substantially contribute to the overall narrative. It was only briefly described in the text and was not essential for conveying the main points. Therefore, we chose to remove the figure to improve clarity.

The resulting INP data (Figure 6 and 7) show a wide range of onset temperatures and INP concentrations. How does this range compare to other studies that measured vertical profiles of INPs?

While direct comparison of onset temperatures is not feasible given their dependence on blank corrections and variability across different techniques, we can compare our results with INP concentrations reported for similar environments. We added the following text to Section 4.2: At −20 °C, the INP concentrations

observed at CRG (0.01–1 L^{-1} in winter; 0.01–12 L^{-1} in summer) and BNF (0.01–1 L^{-1} in spring; 0.02–11 L^{-1} in summer) fall within the broad range reported in recent studies. For example, Creamean et al. (2018) reported 1–11 L^{-1} in springtime agricultural regions in Colorado from vertically-resolved filters via a launched and retrieved balloon system, while similar concentrations (~0.02–12 L^{-1}) were observed by Bieber et al. (2020) and Seifried et al. (2021) near a lake in Austria in summer via UAS. Böhmländer et al. (2025) reported lower values of ~0.2–0.5 L^{-1} during spring and autumn UAS test flights in a boreal environment in Finland. In April in Cyprus, Marinou et al. (2019) reported ~3 L^{-1} from UAS measurements. Values ranging from ~0.2–10 L^{-1} from size-resolved measurements have been reported by Porter et al. (2020) across multiple sites in Europe and the Arctic using balloon-based sampling. Overall, the concentrations reported here are consistent with the range of environments sampled in the literature, spanning relatively clean to more biologically or terrestrially influenced regions.

Bieber, P., Seifried, T. M., Burkart, J., Gratzl, J., Kasper-Giebl, A., Schmale, D. G., and Grothe, H.: A Drone-Based Bioaerosol Sampling System to Monitor Ice Nucleation Particles in the Lower Atmosphere, Remote Sensing, 12, 552, https://doi.org/10.3390/rs12030552, 2020.

Böhmländer, A., Lacher, L., Brus, D., Doulgeris, K.-M., Brasseur, Z., Boyer, M., Kuula, J., Leisner, T., and Möhler, O.: A novel aerosol filter sampler for measuring the vertical distribution of ice-nucleating particles via fixed-wing uncrewed aerial vehicles, Atmospheric Measurement Techniques, 18, 3959–3971, https://doi.org/10.5194/amt-18-3959-2025, 2025.

Creamean, J. M., Primm, K. M., Tolbert, M. A., Hall, E. G., Wendell, J., Jordan, A., Sheridan, P. J., Smith, J., and Schnell, R. C.: HOVERCAT: a novel aerial system for evaluation of aerosol–cloud interactions, Atmospheric Measurement Techniques, 11, 3969–3985, https://doi.org/10.5194/amt-11-3969-2018, 2018.

Marinou, E., Tesche, M., Nenes, A., Ansmann, A., Schrod, J., Mamali, D., Tsekeri, A., Pikridas, M., Baars, H., Engelmann, R., Voudouri, K.-A., Solomos, S., Sciare, J., Groß, S., Ewald, F., and Amiridis, V.: Retrieval of ice-nucleating particle concentrations from lidar observations and comparison with UAV in situ measurements, Atmos. Chem. Phys., 19, 11315–11342, https://doi.org/10.5194/acp-19-11315-2019, 2019.

Porter, G. C. E., Sikora, S. N. F., Adams, M. P., Proske, U., Harrison, A. D., Tarn, M. D., Brooks, I. M., and Murray, B. J.: Resolving the size of ice-nucleating particles with a balloon deployable aerosol sampler: the SHARK, Atmos. Meas. Tech., 13, 2905–2921, https://doi.org/10.5194/amt-13-2905-2020, 2020.

Seifried, T. M., Bieber, P., Kunert, A. T., Iii, D. G. S., Whitmore, K., Fröhlich-Nowoisky, J., and Grothe, H.: Ice Nucleation Activity of Alpine Bioaerosol Emitted in Vicinity of a Birch Forest, Atmosphere, 12, https://doi.org/10.3390/atmos12060779, 2021.

The February vs July comparison in Figure 6 is particularly interesting. Could that correlate with the agricultural activity the authors were discussing earlier? Where any additional test performed on the sample (e.g. heat test) to test for the composition and origin of the INPs?

The characteristic “bio-hump” observed at temperatures warmer than –20 °C in the July spectra, relative to February, is likely associated with agricultural sources. The TBS was deployed in a region bordered by farmland to the east and the Chesapeake Bay to the west, and according to the 2022 USDA Agricultural Census, the dominant crops in Kent County are grains, oilseeds, dry beans, and dry peas (USDA, 2022). The resulting INP spectra are consistent with those observed at SGP, which is similarly influenced by surrounding agricultural activity. Although heat treatments were not performed on these samples, such analyses could help further constrain INP types and may be requested by users through ARM (https://www.arm.gov/guidance/campaign-guidelines/small-campaigns).

We added the following to section 4.2: However, the Baltimore region is bordered by farmland to the east where the dominant crops are grains, oilseeds, dry beans, and dry peas (USDA, 2022), which may have influenced the sampled INP population. Heat treatment

U.S. Department of Agriculture (USDA), National Agricultural Statistics Service (NASS): 2022 Census of Agriculture: County Profile – Kent County, Maryland, available at: https://www.nass.usda.gov/Publications/AgCensus/2022/Online_Resources/County_Profiles/Maryland/cp24029.pdf, last access: 3 April 2026.

We also added the following to section 4.3: Users may request sample collection for total INP concentrations, as well as the application of thermal and peroxide treatments to infer INP types, including heat-labile (likely biological), heat-stable (likely organic), and inorganic (likely mineral) INPs (Barry et al., 2023, 2025; DeMott et al., 2025; Hill et al., 2016; McCluskey et al., 2018; Schiebel et al., 2016; Suski et al., 2018; Testa et al., 2021; Tobo et al., 2019).

Barry, K. R., Hill, T. C. J., Kreidenweis, S. M., DeMott, P. J., Tobo, Y., and Creamean, J. M.: Bioaerosols as indicators of central Arctic ice nucleating particle sources, Atmospheric Chemistry and Physics, 25, 11919–11933, https://doi.org/10.5194/acp-25-11919-2025, 2025.

DeMott, P. J., Mirrielees, J. A., Petters, S. S., Cziczo, D. J., Petters, M. D., Bingemer, H. G., Hill, T. C. J., Froyd, K., Garimella, S., Hallar, A. G., Levin, E. J. T., McCubbin, I. B., Perring, A. E., Rapp, C. N., Schiebel, T., Schrod, J., Suski, K. J., Weber, D., Wolf, M. J., Zawadowicz, M., Zenker, J., Möhler, O., and Brooks, S. D.: Field intercomparison of ice nucleation measurements: the Fifth International Workshop on Ice Nucleation Phase 3 (FIN-03), Atmospheric Measurement Techniques, 18, 639–672, https://doi.org/10.5194/amt-18-639-2025, 2025.

McCluskey, C. S., Hill, T. C. J., Humphries, R. S., Rauker, A. M., Moreau, S., Strutton, P. G., Chambers, S. D., Williams, A. G., McRobert, I., Ward, J., Keywood, M. D., Harnwell, J., Ponsonby, W., Loh, Z. M., Krummel, P. B., Protat, A., Kreidenweis, S. M., and DeMott, P. J.: Observations of ice nucleating particles over Southern Ocean waters, Geophysical Research Letters, 45, 11,989-11,997, https://doi.org/10.1029/2018GL079981, 2018.

Schiebel, T., Höhler, K., Funk, R., Hill, T. C. J., Levin, E. J. T., Nadolny, J., Steinke, I., Suski, K. J., Ullrich, R., Wagner, R., Weber, I., DeMott, P. J., and Möhler, O.: Ice nucleation activity of various agricultural soil

dust aerosol particles, European Geosciences Union General Assembly, Wien, A, April 17-22, 2016. Geophysical Research Abstracts, 18(2016) EGU2016-13422, 2016.

Testa, B., Hill, T. C. J., Marsden, N. A., Barry, K. R., Hume, C. C., Bian, Q., Uetake, J., Hare, H., Perkins, R. J., Möhler, O., Kreidenweis, S. M., and DeMott, P. J.: Ice Nucleating Particle Connections to Regional Argentinian Land Surface Emissions and Weather During the Cloud, Aerosol, and Complex Terrain Interactions Experiment, JGR Atmospheres, 126, https://doi.org/10.1029/2021JD035186, 2021.

Tobo, Y., Adachi, K., DeMott, P. J., Hill, T. C. J., Hamilton, D. S., Mahowald, N. M., Nagatsuka, N., Ohata, S., Uetake, J., Kondo, Y., and Koike, M.: Glacially sourced dust as a potentially significant source of ice nucleating particles, Nat. Geosci., 12, 253–258, https://doi.org/10.1038/s41561-019-0314-x, 2019.

I wish the authors could spend more time discussing the data evaluation of the results from their freezing experiments: It might be worth (i) showing frozen fractions for some samples, at least in the SI, (ii) discussing how the blank background nucleated ice and why background subtraction was applied, and (iii) discussing the choice of calculating confidence intervals using Agresti & Coull[8] over using the approach of Fahy et al.[9] or others.

We agree that additional clarification is valuable.

(i) We do not present frozen fraction curves, as our analysis is based on serial dilutions, with INP concentrations calculated independently for each dilution. As such, frozen fractions are specific to each dilution step rather than representing a single continuous curve, and we instead report INP concentrations derived from these dilution-resolved measurements.

(ii) Blank subtraction is applied to account for residual and procedural sources of INPs. Some INPs may remain on filters even after cleaning and can also be introduced during handling and connection of the sampling units. Additionally, while DI water is filtered (0.1-µm), trace INPs may still remain or be introduced during experimental setup. We also note that defects in PCR trays used for droplet freezing assays can occasionally initiate freezing. Together, these factors contribute to background freezing and necessitate subtraction to isolate the atmospheric INP signal.

(iii) We acknowledge the alternative bootstrap approach proposed by Fahy et al.; however, this method is best suited for datasets with larger droplet counts per distribution (~150–200 droplets). In our case, although ~160 droplets are analyzed per sample, they are partitioned into serial dilutions of 32 wells each, and INP concentrations are derived independently for each dilution. Applying the Fahy et al. approach under these conditions would likely yield overly large and unrepresentative uncertainty bounds. Instead, we use Agresti and Coull confidence intervals, which are appropriate for binomial proportions with sample sizes on the order of ~30, where the central limit theorem supports an approximate normal approximation.

It seems that the authors use the two-sample t-test for determining statistical differences between that samples at different altitudes. Is that test suitable for testing cumulative nucleation spectra? If yes, what values were used for the test? Alternatively, the authors could just discuss the overlapping confidence

intervals or also use a bootstrapping algorithm[9] to back calculate the variations of the ice nucleation measurements.

Because the method of Fahy et al. is best suited for datasets with larger droplet counts per distribution (~150–200 droplets), and the reviewer raised a valid question that a two-sample t-test may not well suited for intercomparison of INP spectra, we now instead use overlapping confidence intervals to assess differences between samples at different altitudes or sites as suggested. The text has been revised accordingly throughout Section 4.2, which can be viewed in the track changes version below.

Summary

What are future improvements that could be made for PUFIN?

We thank the reviewer for this question and the opportunity to outline potential future improvements to PUFIN. At present, altitude measurements rely on the iMet-XQ2, which provides accuracy on the order of ±20 m. Thus, we often instead employ the TBSIMET data, which are more accurate, but it may not be clear to users that this is the best dataset to use. In future iterations, we plan to incorporate a pressure-based altitude reference, which would improve consistency with TBS system measurements and better align with flight logs. We are also considering integration of higher-accuracy GPS sensors (e.g., improving from ~±12 m to sub-meter or centimeter-scale precision available with more advanced systems), as well as implementing a standardized approach to report altitude relative to surface elevation (AGL) directly from flight logs to facilitate inter-site comparisons.

We aim to improve power management in the next-generation design. During some deployments, low battery levels in the iMet-XQ2 may have led to increased power draw as the system attempted to recharge it, potentially impacting overall instrument performance. Future designs will address this by enabling more reliable charging and power distribution to ensure stable operation throughout flights.

Additional, future work should explore a range of rotation times to confirm that 20 minutes is sufficient across filters with varying particle loadings. Our technique has been intercompared with other methods using different particle removal approaches and shows good agreement (DeMott et al., 2017, 2025; Lasher et al., 2024). Nonetheless, future testing to prove the methods is useful.

We have added the following to the Summary section: Future improvements to PUFIN will focus on enhancing altitude accuracy, overall system robustness, and evaluating particle removal methodologies to ensure the most effective approach is used. Planned upgrades include the incorporation of pressure-based altitude measurements and higher-accuracy GPS sensors, as well as standardized reporting of altitude relative to surface elevation (AGL) to facilitate inter-site comparisons. In addition, improvements to power management, particularly more reliable charging and distribution for onboard sensors, are anticipated to ensure stable operation during extended deployments. For particle removal from the filters, this approach has been intercompared with other techniques employing different extraction methods and shows good agreement (DeMott et al., 2017, 2025; Lasher et al., 2024). Future work will evaluate a range of rotation times to ensure that the current 20-minute extraction is sufficient across filters with varying particle loadings.

Minor suggestions:

Line 20: It might be worth dropping two or three concentration levels in the abstract to support the boundary layer stratification and the local vs. transported aerosol argument.

We are not entirely clear on the reviewer's request and have therefore not made changes at this time. We would be happy to address this point if the reviewer can provide further clarification.

Line 34: Change "freezing supercooled liquid …" to "freezing supercooled liquid water …"

Done.

Line 46: Could you perhaps give an example of INP measurements at "surface" and how high these measurements normally extend? It is worth noting that INP measurements from towers can reach sampling heights of 60 m above ground.[10]

We revised the text to read: "However, INP measurements are often made at ground level, which may not accurately represent the concentrations or composition of INP populations at cloud level where ice nucleation processes occur (Burrows et al., 2022)...". Burrows et al. directly addresses this issue, particularly in the context of numerical models, highlighting why this discrepancy is important and why improved representation is needed.

Line 112: It might be worth adding the list and schematic design to the SI of the paper.

While we appreciate the suggestion, we have chosen not to include the current version of the parts list and design in the Supporting Information, as these are subject to change over time. Instead, we prefer to provide the community with access to the most up-to-date parts list and PUFIN design via a GitHub repository, which we will update regularly.

Line 117: It might be worth defining standard liter in "sL min^{-1}".

Done.

Figure 1: Very minor edit, but it seems the mass flow meter symbol does not connect to the airflow arrows correctly.

Fixed.

Table 1: The authors give the altitude of sample in meters above mean sea level (AMSL). Although sampling from 0 to 1000 m AMSL is theoretically possible, it would mean flying from sea level (0 m) to 1000 m. Their sampling locations in Colorado, Alabama and Maryland seem to be already a couple of meters above sea level. The authors should consider adding more accurate sampling heights into Table 1 and also consider adding the GPS coordinates of the sampling locations.

This was a typo in the original submission. The values are AGL, not AMSL, and we have corrected this in Table 1.

Line 217: Consider changing “proportion” to “fraction”

Done.

Line 220: “INP spectra are corrected using DI negative controls and subsequently blank-subtracted.” Please specify what was subtracted, the DI blank or the sample blank (filter from the PUFIN setup).

Both DI and sample blanks are subtracted from the INP spectra. Each sample run includes a 32-well DI negative control. For each 0.5 °C temperature bin, the number of frozen wells in the DI control is subtracted from the number of frozen wells in each dilution. The corrected freezing counts are then converted to frozen fraction for each dilution and subsequently to INP concentration in a combined spectrum.

Sample blanks are processed in a similar manner as filter samples, with INP concentrations calculated per blank filter for each 0.5 °C temperature bin. All blanks from a given campaign are averaged to generate a representative blank spectrum (expressed as INP per blank filter). For each sample, concentrations are first converted to INP per filter, the average blank spectrum is subtracted, and the corrected values are then converted back to INP L^{-1}.

We added the following to Section 3.2: Specifically, each run includes a 32-well DI negative control. For each 0.5 °C temperature bin, the number of frozen wells in the DI control is subtracted from the number of frozen wells in each dilution. The corrected freezing counts are then converted to frozen fraction for each dilution and subsequently to INP concentration as a combined spectrum. Sample blanks are processed in a similar manner as filter samples, with INP concentrations calculated per blank filter for each 0.5 °C temperature bin. All blanks from a given campaign are averaged to generate a representative blank spectrum (expressed as INP per blank filter). For each sample, concentrations are first converted to INP per filter, the average blank spectrum is subtracted, and the corrected values are then converted back to INP L^{-1}.

Line 269: Worth citing the flow rate values of IcePuck for comparison with PUFIN.

We now include the value or range of flow rates for each instrument and deployment in Table 1.

Figure 5: Check the left-hand side of the label, it seems to be cut off. I also got confused with the caption saying “Temperatures at which INPs were detected”. Does that mean onset temperatures, mean freezing temperatures or all temperatures at which droplets froze in the INS experiment?

See comment above. Figure 5 has been removed.

Figure 6: A statement to why and when sampling over an altitude range versus sampling at a set altitude was applied might be useful.

PUFIN sampling is conducted concurrently with other airborne measurements that provide particle size distributions and multimodal micro-spectroscopy, yielding single-particle and molecular-level information on atmospheric aerosols at different altitudes. These complementary measurements predate PUFIN deployment on the ARM TBS and are typically performed within predefined altitude ranges to facilitate comparisons across flight days, seasons, and locations. Although altitude bins are adjusted based on flight conditions and available time, they are generally targeted at ~0–250 m, 250–500 m, and >500 m AGL. As shown in Figures 5 and 6, these ranges were not always strictly followed during the initial PUFIN flights due to operational constraints. We updated the figure legends to reflect the correct start and end altitudes based on TBSIMET data, which are more accurate and available through the ARM Data Center (Dexheimer et al., 2024).

We added new text on sampling strategy in Section 2.4.2: PUFIN sampling is often conducted in coordination with concurrent airborne measurements, including aerosol size distributions and multimodal micro-spectroscopy, to enable complementary characterization of aerosol properties across altitudes. Sampling is performed within predefined altitude ranges to facilitate comparison across flights, seasons, and locations, targeting roughly 0–250 m, 250–500 m, and >500 m AGL. These altitude bins are adjusted as needed based on flight duration and atmospheric conditions. They can be modified in real time to target layers of interest identified from on-site aerosol and meteorological measurements.

We also added the following to Section 2.2: However, these measurements are only accurate to approximately ±20 m; therefore, altitude data are taken from the TBS iMet system, available as the "TBSIMET" datastream from the ARM Data Center (Dexheimer et al., 2024).

Line 341: Is the "concentrations as low as 10^{-2} INP L-^{1} in as little as 28 minutes" also tied to a minimum onset temperature? I guess with the current workflow, 10^{-2} INP L^{-1} active below -30°C would not be detectable. Consider attaching a minimal onset temperature to this statement.

The minimum onset temperatures are constrained by INP contributions from blank filters and DI water backgrounds, in addition to the collection times. To accurately report and intercompare onset temperatures, all of these factors would need to be consistent. As this is not always the case, particularly with variability in the blanks, we are unable to robustly report this value.

This is very picky, but the authors use "warmer temperature" quite frequently. Technically, an object like a droplet can be warm, however, the temperature is a property of the object and therefore either high or low, not warm or cold.

We appreciate the reviewer's point and revised the six instances where we used "warmer freezing temperatures." We retained one instance of "warm-temperature INPs," as this is a commonly used term within the ice nucleation community.

It might be worth considering including PUFIN in the title for further papers referencing the technique. Suggestion: "Reaching new heights: Profiling Upper altitudes For Ice Nucleation (PUFIN) on the Atmospheric Radiation Measurement (ARM) tethered balloon systems"

Thank you for the suggestion – a valid point. We adopted the reviewer's proposed title.

Line 350: Again, great job and big step to help the ice nucleation community with access to INP measurements.

Thank you!

References:

1. Schmale Iii, D. G.; Dingus, B. R.; Reinholtz, C. Development and Application of an Autonomous Unmanned Aerial Vehicle for Precise Aerobiological Sampling above Agricultural Fields. J. Field Robot. 2008, 25 (3), 133–147. https://doi.org/10.1002/rob.20232.
2. Borchers, C.; Moormann, L.; Geil, B.; Karbach, N.; Wasserzier, D.; Hoffmann, T. Development and Use of a Lightweight Sampling System for Height-Selective UAV-Based Measurements of Organic Aerosol Particles. Atmospheric Meas. Tech. 2025, 18 (23), 7231–7242. https://doi.org/10.5194/amt-18-7231-2025.
3. Bieber, P.; Seifried, T. M.; Burkart, J.; Gratzl, J.; Kasper-Giebl, A.; Schmale, D. G.; Grothe, H. A Drone-Based Bioaerosol Sampling System to Monitor Ice Nucleation Particles in the Lower Atmosphere. Remote Sens. 2020, 12 (3), 552. https://doi.org/10.3390/rs12030552.
4. Seifried, T. M.; Bieber, P.; Kunert, A. T.; Schmale, D. G.; Whitmore, K.; Fröhlich-Nowoisky, J.; Grothe, H. Ice Nucleation Activity of Alpine Bioaerosol Emitted in Vicinity of a Birch Forest. Atmosphere 2021, 12 (6), 779. https://doi.org/10.3390/atmos12060779.
5. Porter, G. C. E.; Sikora, S. N. F.; Adams, M. P.; Proske, U.; Harrison, A. D.; Tarn, M. D.; Brooks, I. M.; Murray, B. J. Resolving the Size of Ice-Nucleating Particles with a Balloon Deployable Aerosol Sampler: The SHARK. Atmospheric Meas. Tech. 2020, 13 (6), 2905–2921. https://doi.org/10.5194/amt-13-2905-2020.
6. Böhmländer, A. J.; Lacher, L.; Brus, D.; Doulgeris, K.-M.; Brasseur, Z.; Boyer, M.; Kuula, J.; Leisner, T.; Möhler, O. A Novel Aerosol Filter Sampler for Measuring the Vertical Distribution of Ice-Nucleating Particles via Fixed-Wing Uncrewed Aerial Vehicles. September 4, 2024. https://doi.org/10.5194/amt-2024-120.
7. Šantl-Temkiv, T.; Amato, P.; Gosewinkel, U.; Thyrhaug, R.; Charton, A.; Chicot, B.; Finster, K.; Bratbak, G.; Löndahl, J. High-Flow-Rate Impinger for the Study of Concentration, Viability, Metabolic Activity, and Ice-Nucleation Activity of Airborne Bacteria. Environ. Sci. Technol. 2017, 51 (19), 11224–11234. https://doi.org/10.1021/acs.est.7b01480.
8. Agresti, A.; Coull, B. A. Approximate Is Better than "Exact" for Interval Estimation of Binomial Proportions. Am. Stat. 1998, 52 (2), 119–126. https://doi.org/10.1080/00031305.1998.10480550.
9. Fahy, W. D.; Shalizi, C. R.; Sullivan, R. C. A Universally Applicable Method of Calculating Confidence Bands for Ice Nucleation Spectra Derived from Droplet Freezing Experiments. Atmospheric Meas. Tech. 2022, 15 (22), 6819–6836. https://doi.org/10.5194/amt-15-6819-2022.
10. Schrod, J.; Thomson, E. S.; Weber, D.; Kossmann, J.; Pöhlker, C.; Saturno, J.; Ditas, F.; Artaxo, P.; Clouard, V.; Saurel, J.-M.; Ebert, M.; Curtius, J.; Bingemer, H. G. Long-Term Deposition and Condensation Ice-Nucleating Particle Measurements from Four Stations across the Globe. Atmospheric Chem. Phys. 2020, 20 (24), 15983–16006. https://doi.org/10.5194/acp-20-15983-2020.

Reaching new heights: Profiling Upper altitudes For Ice Nucleation (PUFIN) on the Atmospheric Radiation Measurement (ARM) tethered balloon systems

Deleted: A vertically-resolved ice nucleating particle sampler operating

Jessie M. Creamean[1], Darielle Dexheimer[2], Carson C. Hume[1], Maria Vazquez[1], Benjamin T. M. Hess[2], Casey M. Longbottom[2], Carlos A. Ruiz[2], Adam K. Theisen[3]

[1]Department of Atmospheric Science, Colorado State University, Fort Collins, Colorado, 80523, USA

[2]Sandia National Laboratory, Albuquerque, New Mexico, 87123, USA

[3]Argonne National Laboratory, Lemont, Illinois, 60439, USA

Correspondence to: Jessie M. Creamean (jessie.creamean@colostate.edu)

Abstract

Ice nucleating particles (INPs) are a rare yet climatically relevant subset of aerosols that initiate ice formation in mixed-phase clouds, strongly influencing cloud microphysics, precipitation, and Earth's radiative balance. Despite their significance, ground-based measurements of INPs may not always be representative of those at cloud level, yet vertically-resolved INP measurements remain limited. Here, we introduce PUFIN (Profiling Upper altitudes For Ice Nucleation), a robust, lightweight INP sampler designed for routine deployment on the U.S. Department of Energy Atmospheric Radiation Measurement (ARM) user facility's tethered balloon system (TBS). PUFIN collects multiple filter samples per flight at up to three altitudes, integrating real-time monitoring of flow, power consumption, and atmospheric conditions, while remaining fully operable from the ground. Multiple deployments at two ARM observatories in Maryland and Alabama demonstrate that PUFIN achieves sufficient aerosol loading to detect INPs down to ~10^{-3} L^{-1} within as little as 28 minutes of sampling, but typically within an hour. Data from recent deployments reveal altitude-dependent variability in INP concentrations, indicative of boundary layer stratification and contributions from both local and transported aerosol sources. All resulting TBSINP data are publicly available via the ARM Data Center, and researchers may request PUFIN for future TBS campaigns or access archived filters for additional analyses. Looking forward, routine PUFIN deployments can be used to enhance understanding of the vertical distribution and seasonal variability of INPs, enabling improved representation of aerosol-cloud interactions in Earth system models and advancing predictive capabilities for weather and climate.

Short summary

PUFIN (Profiling Upper altitudes For Ice Nucleation) is a lightweight sampler flown on the U.S. Department of Energy's Atmospheric Radiation Measurement user facility's tethered balloons to measure ice nucleating particles at multiple altitudes. Deployments in Maryland and Alabama show it can detect low concentrations in under an hour and capture changes

with height. All data are publicly available, and future flights will help track seasonal and vertical patterns of these unique particles.

1 Introduction

Ice nucleating particles (INPs) are a rare, but critical subset of atmospheric aerosols that catalyze the formation of cloud ice through heterogeneous nucleation, i.e., freezing supercooled liquid water at temperatures above the homogenous threshold at roughly –38 °C (Pruppacher and Klett, 2010). Despite existing at concentrations orders of magnitude lower than cloud condensation nuclei (CCN) that facilitate the formation of cloud droplets, INPs exert an outsized influence on cloud microphysics, lifetime, and radiative properties (Kanji et al., 2017), especially in mixed-phase clouds, which are arguably the most prominent type of cloud globally (Mülmenstädt et al., 2015). By initiating the glaciation of such clouds, INPs can accelerate precipitation processes, alter cloud reflectivity, and modulate the hydrological cycle. Their role in determining cloud phase is especially consequential for Earth's energy balance, as ice-containing clouds differ strongly from liquid-only clouds in albedo and longwave emissivity (Storelvmo, 2017). Therefore, understanding INP abundance, composition, and variability is essential for improving the representation of aerosol-cloud interactions in weather and Earth system models (Burrows et al., 2022).

INPs connect boundary layer processes to terrestrial, oceanic, and cryospheric sources, linking biogeochemical systems to climate feedbacks on regional to global scales (Creamean et al., 2025b; Murray et al., 2021; Schnell and Vali, 1976; Steiner, 2020). However, INP measurements are often made at ground level, which may not accurately represent the concentrations or composition of INP populations at cloud level where ice nucleation processes occur (Burrows et al., 2022), and are only directly relevant when clouds are coupled to the surface (e.g., Griesche et al., 2021). Furthermore, the types of INPs often vary with altitude. A recent modeling study suggests that, on a global average, biological and marine organic INPs are more prevalent at lower altitudes depending on hemisphere and freezing temperature, whereas dust INPs dominate at higher altitudes (Chatziparaschos et al., 2025). While crewed aircraft have a long history of conducting airborne INP measurements, they typically provide only brief snapshots and often cannot sample close enough to the surface to capture the full vertical structure from the ground to cloud base.

Deleted: the surface

Smaller platforms such as uncrewed aerial and tethered balloon systems (UASs and TBSs, respectively) help fill this gap. Although these systems cannot accommodate the larger payloads of crewed aircraft, advances in lightweight instrumentation now enable vertically-resolved comprehensive measurements of meteorology and aerosol properties (Dexheimer et al., 2024; Mei et al., 2025; Pohorsky et al., 2024; Pilz et al., 2022). TBSs are particularly valuable because they can provide routine profiling or sustained sampling of aerosols at targeted altitudes up to several hours, reaching up to 1–2 km above ground level, below, into, and above clouds (e.g., Creamean et al., 2021). These capabilities offer certain advantages over UASs, which are frequently limited by line-of-sight or altitude regulations, payload weight restrictions depending on aircraft design,

and relatively short flight times at often an hour or less. Recent studies such as Pilz et al. (2023, 2024) and Londardi et al. (2022) reported aerosol observations from TBS platforms during summer of the 2019–2020 Multidisciplinary drifting Observatory for the Study of Arctic Climate (MOSAiC) expedition. Their results revealed substantial complexity in aerosol vertical structure, which varied by day and airmass origin, though most profiles indicated new particle formation above low-level clouds. Similarly, Guy et al. (2024) measured aerosol size distributions from the surface to cloud base over the central Greenland Ice Sheet using TBS and found distinct stratification, concluding that surface measurements alone failed to represent cloud-relevant aerosol conditions roughly half of the time. Pohorsky et al. (2025) also observed distinct aerosol layering using TBS in a high-latitude urban environment, where heavy pollution was trapped beneath a strong temperature inversion and overlain by typical Arctic haze aerosols. In another study, Zinke et al. (2021) developed a cloud water sampler they deployed on a TBS, enabling measurements of bulk cloud residual chemical composition and INP concentrations in the high Arctic from an icebreaker, although these were not vertically-resolved.

Only a limited number of studies have reported on vertically-resolved INP measurements from balloon or UAS platforms. Creamean et al. (2018) quantified INPs in both immersion and deposition modes across six altitude ranges during three test flights in Colorado, using launched balloons rather than a TBS. This approach was challenging, as launched balloons can be entrained in low-level jets carrying them long distances, and physical retrieval is required to collect filters for offline INP analysis. Bieber et al. (2020) and Seifried et al. (2021) describe a developed system, the DAPSI (Drone-based Aerosol Particle Sampling Impinger/Impactor), for collecting INP samples using UAS. To date, results have been limited to test flights and a short (3-day) campaign conducted near a lake in Austria during summer. Porter et al. (2020) developed a size-resolved sampling payload for offline INP analysis, the SHARK (Selective Height Aerosol Research Kit), for deployment on a TBS. This system has been tested at several locations, including in the high Arctic (Porter et al., 2022); however, it collects samples at only one altitude above ground level per flight. More recently, Böhmländer et al. (2025) developed an INP sampler capable of collecting filters at multiple altitudes for offline analysis. The system was initially tested on a UAS in Finland, with plans to test it for TBS applications. While these previous studies mark important progress toward resolving the vertical distribution of INPs, substantial effort is still needed to establish reliable, routine measurements. Such advancements are essential for improving the representation of INPs in models and, consequently, the simulation of aerosol-cloud interactions across vertical scales.

Here, we present a robust INP sampling system designed to address this gap, called PUFIN: Profiling Upper altitudes For Ice Nucleation. The instrument collects filters at up to three distinct altitudes plus a blank during each TBS flight and can be fully controlled from the ground. Developed collaboratively by the INP and TBS instrument teams under the U.S. Department of Energy's Atmospheric Radiation Measurement (DOE ARM) user facility, the system is intended for routine deployment at ARM sites in response to user requests. Resulting data products are publicly released on the ARM Data Center (https://www.arm.gov/data) within six months of each TBS campaign. In this paper, we describe the system design and flight

operations, outline the offline sample processing and data production, summarize the data that are currently available and how to access them, and guide users how to request deployment of PUFIN for their own research needs.

2 Instrument description

2.1 DOE ARM TBS and INP initiatives

The ARM TBS program has evolved into a critical observational capability for capturing high-resolution, vertically-stratified atmospheric data, operating at ARM observatories using helium-filled Skydoc balloons capable of ascending to approximately 1.5 km above ground level. Typically, ARM conducts six to eight two-week TBS missions each year, with flights deploying baseline instrumentation suites, including aerosol, thermodynamic, and turbulence sensors, tailored to research objectives across clear-air and, occasionally, in-cloud conditions. More details on the TBS system and standard instrument payload can be found in Dexheimer et al. (2024) and up-to-date information on the ARM TBS website (https://www.arm.gov/capabilities/instruments/tbs).

Since 2020, ARM has provided routine, publicly-available INP measurements at select sites. Prior to that, INP sampling was considered a guest instrument activity and required proposals by researchers for targeted campaigns and locations. Demand for such measurements has since grown, and as of 2025 INP data are available from seven ARM sites. These data are generated by collecting filters at ARM fixed observatories and mobile facilities, followed by offline processing with the Ice Nucleation Spectrometer (INS) at Colorado State University (CSU), as described briefly below and in detail in Creamean et al. (2024, 2025a). Data products can be accessed through the ARM Data Center by searching for "INP." Up-to-date information, including deployment details and data availability from TBS operations, is provided on the ARM INS website (https://www.arm.gov/capabilities/instruments/ins), where a routinely updated field log is also available for community reference.

2.2 Design and integration of PUFIN with the TBS

PUFIN operates similarly to the standard ARM INP sampling system, but on a smaller scale and with multiple filters attached. A detailed parts list and design schematic are publicly available on GitHub at https://github.com/ARM-Development/TBS-INP-Design to enable researchers to build and deploy their own PUFIN replicas for their independent or collaborative studies. Figure 1 illustrates PUFIN's flow diagram, which includes a dry floating scroll pump (SVF-E0-50P, ScrollLabs®), a multi-gas flow sensor (SFM4300, Sensirion AG), four stainless steel solenoid valves (PL-220101, Plum Garden), and four ports for reusable 47-mm in-line polycarbonate filter holders (Pall Life Sciences). The pump features a brushless motor powered by 24 VDC, achieves an ultimate vacuum of <1 mbar, and provides flow rates up to 50 sL min^{-1} (liters per minute at standard temperature and pressure (STP): 0°C and 101.32 kPa) without a filter attached. The flow sensor operates over a 0–50 sL min^{-1} range. Each solenoid valve, with ¼-inch threaded inlet connections, requires 12 VDC and is controlled via a motor driver

controller board (L298N, HiLetGo). The filter holders, with an effective filtration area of 9.6 cm², are prepared as outlined in Section 2.4.1. With prepared filter holders attached, the pump can pull a maximum of roughly 11 sL min^{-1} through the standard 0.2-µm pore size filters used for the ARM INP measurements. Connections at both ends consist of ¼-inch hose barb adapters, linking to ¼-inch tubing inside PUFIN and opening directly to the air on the exterior (Figure 2). PUFIN's components are protected by a 3D-printed enclosure, which is equipped with a ventilation fan for in-flight cooling and backed with a 0.32 cm thick aluminum electrical ground distribution board that also provides structural integrity for the mounting point to the tether. The enclosure and all other 3D-printed parts are fabricated from white ASA (acrylonitrile styrene acrylate) polymer (Bambu Lab) due to its exceptional UV and temperature resistance, high impact strength, durability, and suitability for long-term outdoor use. The total flight-ready weight of the instrument is 6.1 kg.

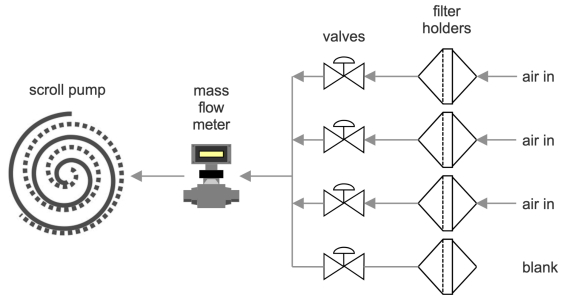

Figure 1: Schematic of PUFIN airflow. Main components are labeled. Valves are sequentially triggered to direct airflow through one filter at a time, while the fourth filter serves as a field blank and remains closed to airflow. Arrows indicate direction of airflow. The schematic was generated with SmartDraw.com.

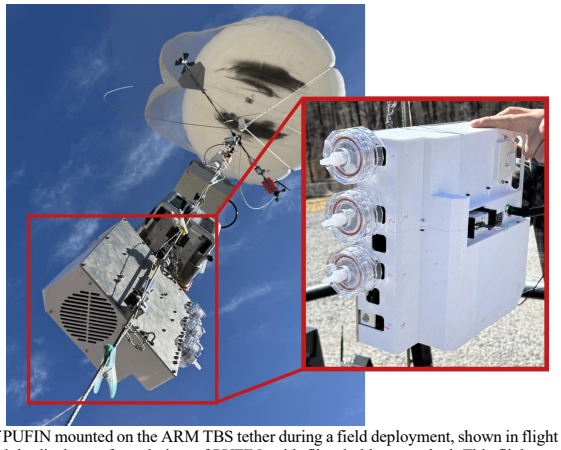

Figure 2: Exterior views of PUFIN mounted on the ARM TBS tether during a field deployment, shown in flight alongside other instrument payloads. The inset on the right displays a frontal view of PUFIN with filter holders attached. This flight required collection of INPs at two designated altitudes plus one field blank.

Figure 3 illustrates the primary components and features of both the interior and immediate exterior of PUFIN. It is powered by a 28.8-V, 14,000-mAh lithium ion battery pack (8S4P, MaxAmps), housed within a 3D-printed enclosure for protection and secure mounting. The battery pack typically powers PUFIN for approximately 3.5 hours depending on the target flow rate, ambient temperature, and air density. A 30-W DC/DC converter (PYB30-U, Bel Power Solutions) steps down the battery voltage to 12 V to supply the pump, valves, and sensors. System power consumption is monitored using a current, voltage, and power monitor (INA260, Adafruit Industries LLC), providing measurements of electrical load and enabling safe operation during flight. PUFIN's control system is built around a TEENSY 4.1 microcontroller (iMXRT1062, SparkFun Electronics), which serves as the central processing unit for all sensor operations. Onboard sensors communicate digitally with the microcontroller, and analog pump command signals are generated using a digital-to-analog converter (MCP4725, SparkFun Electronics), enabling the microcontroller and other computational components to interpret and respond to sensor inputs accurately. This configuration allows precise regulation of flow rates, valve actuation, and system monitoring during flight. PUFIN's communications system integrates atmospheric sensing, data transmission, and user interface components to enable real-time monitoring during flight. An iMet-XQ2 sensor measures atmospheric pressure, temperature, and humidity, and includes a GPS receiver, rechargeable battery, and onboard data logger. However, these measurements are only accurate to approximately ±20 m; therefore, altitude data are taken from the TBS iMet system, available as the "TBSIMET" datastream from the ARM Data Center (Dexheimer et al., 2024). The sensor is mounted in a custom 3D-printed holder bracket. Wireless data transmission is achieved via a 2.4-GHz radio frequency transceiver module with antenna (NRF24L01P+PA+LNA, HiLetgo), allowing real-time communication between PUFIN and the ground station. A 9-dBi

omni-directional antenna is used with the transceiver to increase range (ANT-WS-A-NF-09-150, ATOP Technologies). System status and measurements are displayed locally on a 2.8-inch LCD touch panel (ILI9341, HiLetgo) and a digital LED tube clock module. All remote electronics, including the transceiver, display, and sensor assemblies, are housed in a series of 3D-printed enclosures to protect components while maintaining accessibility and visibility during deployment.

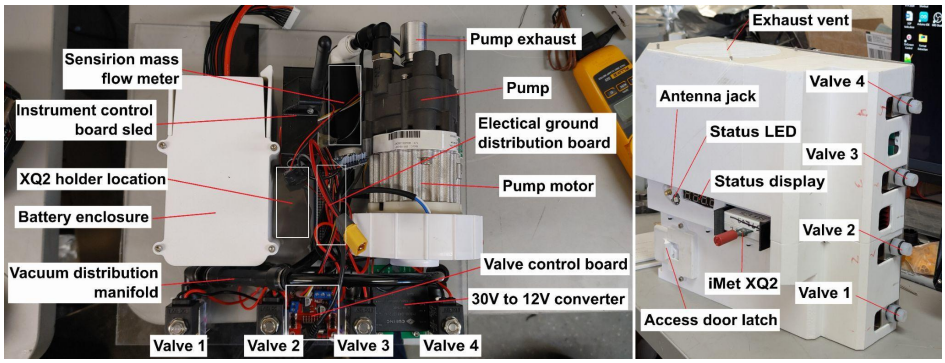

Figure 3: Photos of the interior (left) and immediate exterior (right) of PUFIN. The main components and features are labeled. The exterior housing shown in the right image is-3D printed.

2.4 INP sample collection during deployments

2.4.1 Filter material and holder preparation

In preparation for aerosol collection, 0.2-µm polycarbonate filters (47-mm diameter Whatman® Nuclepore™ Track-Etched Membranes) are loaded into the reusable 47-mm polycarbonate in-line filter holder, pre-cleaned with cycles of methanol and deionized water. These filters are identical in preparation to those used at ARM fixed and mobile sites (Creamean et al., 2025a). All components, including filters, forceps, and workspaces are pre-cleaned following the procedure described in Barry et al. (2021). Filter holders are disassembled and reassembled under ultraclean conditions inside a laminar flow cabinet with near-zero ambient particle concentrations, wrapped in foil, then sealed and stored individually in clean airtight bags until deployment. Filter holders are thoroughly cleaned following each use and before reuse by immersion in 5% hydrogen peroxide for 1 hour, followed by 10 minutes of ultra sonication in deionized water and Windex® Original Glass Cleaner to remove any remaining particles.

The 0.2-µm filters used in PUFIN provide a simple, robust, and widely adopted approach for INP sampling, enabling bulk-integrated collection across particle sizes and facilitating intercomparability across studies. Compared to impingers, filters do not require liquid handling, are less sensitive to environmental conditions, and allow for more stable storage of INPs when frozen (e.g., Beall et al., 2020). Compared to impactors, they provide a bulk-integrated sample rather than size-segregated

Formatted: Space After: 0 pt

fractions, simplifying analysis and reducing uncertainties associated with particle bounce and stage-specific collection efficiencies. Based on calculations from Spurny and Lodge (1972), these filters exhibit relatively high collection efficiencies across PUFIN's operating flow rate range (4-11 L min^{-1}), with a decrease near 150 nm but still maintaining efficiencies on the order of 78–91%. In principle, the filters sample total suspended particulates. However, inlet-related biases, particularly for coarse particles, may arise due to wind speed-dependent inertial and gravitational losses (e.g., governed by Stokes number and settling velocity), such that the largest particles may be underrepresented, although this has not yet been empirically quantified for this system.

Formatted: Superscript

2.4.2 Operation of PUFIN during flight

PUFIN is typically operated manually unless used in environments with elevated electromagnetic interference. During setup, the blank filter remains installed as the instrument is mounted onto the tether. It is then removed using latex gloves, wrapped in aluminum foil, labeled, and stored in a –80 °C ultracold freezer. The pump is activated, and the first solenoid valve is manually opened to begin sampling (Figure 4). The instrument makes multiple passes through the first target altitude over a 30–60 minute interval. Before transitioning to the next altitude range, the valve is closed, and the next solenoid valve is opened. This process is repeated for the third valve at the highest altitude.

PUFIN sampling is often conducted in coordination with concurrent airborne measurements, including aerosol size distributions and multimodal micro-spectroscopy, to enable complementary characterization of aerosol properties across altitudes. Sampling is performed within predefined altitude ranges to facilitate comparison across flights, seasons, and locations, targeting roughly 0–250 m, 250–500 m, and >500 m AGL. These altitude bins are adjusted as needed based on flight duration and atmospheric conditions. They can be modified in real time to target layers of interest identified from on-site aerosol and meteorological measurements.

After the flight, the instrument is removed from the tether and placed on a workspace lined with clean aluminum foil. Filters are removed using latex gloves, wrapped in foil, labeled, and stored in the same plastic bag as the blank filter in the –80 °C freezer. The operation log is retrieved from the onboard SD card. Once all flights are completed, the collected filters are shipped overnight to CSU for analysis in a hard-sided 7 kg-capacity cooler with 2.2 kg of dry ice.

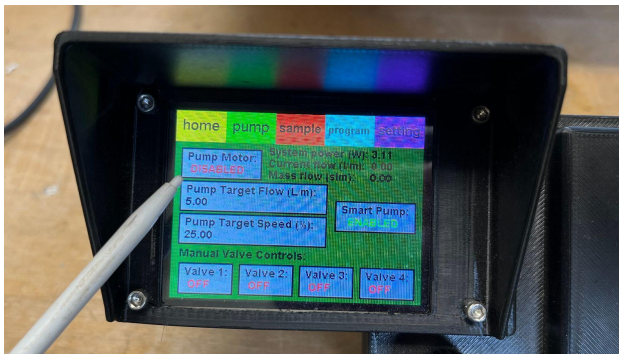

Figure 4: Photo of the PUFIN ground station undergoing manual operation. The image depicts the pump motor in an inactive state ('DISABLED') with all four valves closed and 0 sL min^{-1} of flow. The target flow upon activation is 5.00 sL min^{-1}.

3 Filter processing for INP data

3.1 INS sample processing

The INS, similar to the CSU Ice Spectrometer, simulates immersion freezing of cloud droplets by measuring heterogeneous ice nucleation initiated by ambient aerosol particles acting INPs (Creamean et al., 2024, 2025a). This technique provides quantitative insight into the population of ambient aerosols capable of initiating cloud ice formation across a broad range of subzero temperatures, thereby determining INP concentrations spanning up to six orders of magnitude. The INS is supported by robust experimental protocols and has been widely applied across diverse atmospheric contexts (e.g., Barry et al., 2023; Beall et al., 2017; DeMott et al., 2017; Hill et al., 2016; Hiranuma et al., 2015; Lacher et al., 2024; McCluskey et al., 2017; Suski et al., 2018).

The INS contains two units that operate simultaneously to increase processing throughput. Each unit consists of two 96-well aluminum incubation blocks designed for polymerase chain reaction (PCR) plates, arranged end-to-end and thermally regulated via cold plates on the sides and base. The instrument measures freezing across a temperature range of 0 °C to approximately –27 to –30 °C. For analysis, filters are carefully removed from the in-line holders under ultraclean conditions inside a laminar flow cabinet. Each filter is placed in a sterile 50 mL polypropylene tube with 7–10 mL of 0.1 µm-filtered deionized (DI) water, with the volume adjusted based on expected aerosol loading; lower volumes are used for cleaner environments to enhance sensitivity. Samples are re-suspended by end-over-end rotation for 20 minutes. Serial dilutions are prepared using the suspensions and 0.1 µm-filtered DI water, typically including 11-fold dilution steps. Each suspension and its dilutions are aliquoted into sets of 32 wells (50 µL per well) of single-use 96-well PCR trays (Optimum Ultra), along with a 32-well negative control containing only filtered DI water. Trays are placed into the INS blocks and cooled at a controlled

rate of 0.33 °C min^{-1}. Uncertainty of the thermocouple is ±0.2 °C. Freezing is monitored optically using a CCD camera with a 1-second resolution. A continuous flow of HEPA-filtered N_2, precooled just above block temperature, purges the headspace to minimize condensation and prevent warming of the samples. Field blanks are processed in an identical manner as sampled filters.

3.2 INP concentration and uncertainty calculations

INP concentrations, blank corrections, and uncertainties were generated using the Open-source Library for Automating Freezing Data acQuisition from Ice Nucleation Spectrometer (OLAF DaQ INS; https://github.com/SiGran/OLAF). Details are described in Creamean et al. (2025a). The program calculates INP concentrations at each temperature interval using the fraction of frozen droplets and the known total volume of air that passed through each filter, following Equation (1) (Vali, 1971):

$$K(\theta)\ (L^{-1}) = -\frac{ln\ (1-f)}{Vdrop} \times \frac{Vsuspension}{Vair} \quad (1)$$

where f is the fraction of frozen droplets, V_{drop} is the volume of each droplet, $V_{suspension}$ is the volume of the suspension, and V_{air} is the volume of air sampled (liters at STP of 0 °C and 101.32 kPa). The primary variable of the INS is the freezing temperature spectrum of cumulative immersion mode INP number concentration, $K(\theta)$, from aerosols re-suspended from individual filters. INP spectra are corrected using DI negative controls and subsequently blank-subtracted. Specifically, each run includes a 32-well DI negative control. For each 0.5 °C temperature bin, the number of frozen wells in the DI control is subtracted from the number of frozen wells in each dilution. The corrected freezing counts are then converted to frozen fraction for each dilution and subsequently to INP concentration as a combined spectrum. Sample blanks are processed in a similar manner as filter samples, with INP concentrations calculated per blank filter for each 0.5 °C temperature bin. All blanks from a given campaign are averaged to generate a representative blank spectrum (expressed as INP per blank filter). For each sample, concentrations are first converted to INP per filter, the average blank spectrum is subtracted, and the corrected values are then converted back to INP L^{-1}. Binomial 95% confidence intervals are calculated following Agresti and Coull (1998), varying with the proportion of wells frozen. For example, freezing in 1 of 32 wells yields a confidence interval range of approximately 0.2–5.0 times the estimated concentration, while 16 of 32 yields approximately 0.7–1.3 times the estimated concentration. $K(\theta)$ and upper and lower confidence intervals are derived per every 0.5 °C interval.

Deleted: proportion

Deleted: standard temperature and pressure (

Deleted:)

Formatted: Superscript

4 Accessibility of PUFIN and resulting TBSINP data

4.1 Availability of TBSINP data and filters

INP data collected with PUFIN on the ARM TBS and processed using the INS are available through the ARM Data Center by searching for "TBSINP". Not all TBS deployments included PUFIN and resulted in TBSINP data, but this section summarizes those that have. Table 1 provides an overview of TBS campaign details through the end of 2025, which occurred

at four main ARM sites: 1) Southern Great Plains (314 m AMSL, 36.607° N, 97.488° E), 2) Gunnison, Colorado (2886 m AMSL, 38.956° N, 106.988° W) during the SAIL (Surface Atmosphere Integrated field Laboratory) campaign, 3) Bankhead National Forest, Alabama (293 m AMSL, 34.342° N, 87.338° W), and 4) Baltimore, Maryland (158 m AMSL, 39.422° N, 77.21° W) during the CouRAGE (Coastal-urban-Rural Atmospheric Gradient Experiment) campaign. While not all datasets are available, those pending release as of the publication date of this paper are indicated in the table. Campaigns that used an earlier INP collection method predating PUFIN (called the IcePuck), as described in Creamean et al. (2024), are also identified. Limitations of the IcePuck in collecting sufficient air volumes to capture the higher freezing temperature range of the cumulative INP spectrum, along with challenges in ease of use, prompted the development of PUFIN. Exact start and end dates and times, altitude range, sample duration, and volume of air sampled for each sample and each flight can be found in the field log link on the INS website (https://www.arm.gov/capabilities/instruments/ins). For deployments in which data are not or only partially available, researchers interested in accessing or analyzing these samples may submit a request to ARM (https://www.arm.gov/guidance/campaign-guidelines/small-campaigns). User-requested data from additional INP processing will also be made accessible to the broader research community through the ARM Data Center.

Table 1. Details on ARM TBS deployments with INP sampling. Information includes ARM sampling site, flight dates during each deployment, altitude range of the flights (meters above mean sea level), the range of sample duration (minutes), value or range of flow rates during sample collection (L min^{-1}), range of volume of air collected per sample (liters), if the data are available on the ARM Data Center (ADC), and the sampling method used. For the site, SGP = Southern Great Plains, GUC = Gunnison, Colorado, BNF = Bankhead National Forest, Alabama, and CRG = Baltimore, Maryland. Sampling method indicates whether the older INP sampler (IcePuck) or PUFIN were used. For data availability, yes = all data are posted, partial = some data are available within the dates indicated, queued = samples will be processed / data will be available in the future, and no = samples are archived for possible future processing / no data are available.

ARM site	Flight dates	Altitude range (m AGL)	Sample duration (min)	Flow rate (L min^{-1})	Vol air sampled (L)	Data on ADC	Sampling method
SGP	10 – 26 Apr 2022	0 – 1000	30 – 150	0.3 – 0.9	34 – 133	Yes	IcePuck
GUC	6 – 16 May 2022	0 – 500	74 – 149	0.6	40 – 90	Yes	IcePuck
GUC	23 – 28 Jul 2022	0 – 750	21 – 119	0.6	27 – 71	Partial	IcePuck
GUC	21 – 24 Jan 2023	0 – 560	33 – 74	0.4 – 0.5	30 – 37	No	IcePuck
GUC	6 – 11 Apr 2023	0 – 1150	70 – 120	0.1 – 0.5	34 – 133	Partial	IcePuck
GUC	9 – 13 May 2023	0 – 500	119 – 120	0.3 – 0.5	30 – 41	No	IcePuck
GUC	9 – 15 Jun 2023	0 – 1000	60 – 120	0.3 – 0.5	16 – 47	No	IcePuck
CRG	14 – 23 Feb 2025	0 – 900	59 – 119	7.1 – 11.0	447 – 1456	Yes	PUFIN
CRG	15 – 28 Jul 2025	0 – 1050	4 – 30	4.6 – 8.2	31 – 245	Yes	PUFIN

Deleted: warmer

Formatted: Superscript

Inserted Cells

Deleted: AMSL

Formatted: Superscript

BNF	21 – 27 Mar 2025	0 – 1100	60 – 91	6.9 – 7.2	416 – 1157	Yes	PUFIN
BNF	17 – 27 Apr 2025	0 – 850	46 – 62	6.9 – 7.3	350 – 438	Yes	PUFIN
BNF	29 May – 6 Jun 2025	0 – 700	28 – 44	7.3 – 8.9	204 – 394	Yes	PUFIN
BNF	9 – 24 Aug 2025	0 – 850	30 – 89	7.7 – 8.9	254 – 713	Yes	PUFIN

Deleted: Queued

The SGP site is located in the midst of agricultural fields in north-central Oklahoma, United States, which often produce high concentrations of INPs from soil dust lofted during farming activities such as harvesting and plowing (Knopf et al., 2021). The TBS deployment at SGP was part of an intensive observational period (IOP) aimed at investigating the drivers of variability in INP concentrations from regional emissions of fertile, organic-rich agricultural soils, as well as intermittent contributions from other sources, including aerosols from controlled burns or wildfires, long-range transported desert dust, cellulose-containing plant matter, fungal spores, and microbial particles. Cornwell et al. (2024) reported enrichments of phosphate, lead, and soil organics in dust particles acting as INPs from surface measurements, while non-ice-nucleating aerosols were primarily carbonaceous or secondary in origin. TBSINP data from this deployment are still under analysis for a forthcoming publication, but several noteworthy case days have already emerged, including instances with elevated particle concentration layers within the boundary layer. The GUC site, part of the SAIL campaign, is located high in the Colorado Rocky Mountains. SAIL aimed to develop a quantitative understanding of atmospheric and land–atmosphere interaction processes, across relevant scales, that influence mountain hydrology in the midlatitude continental interior of the United States (Feldman et al., 2023). TBS flights at GUC were conducted in all seasons except autumn and sampled both within the mountain valley and above ridgelines, capturing cases influenced by local valley sources as well as more regional aerosol below cloud level.

Deleted: (Figure 5)

Deleted: However, Figure 5 also includes data from SGP and GUC sites, so some of the observed variability likely reflects the distinct aerosol loadings characteristic of each location.

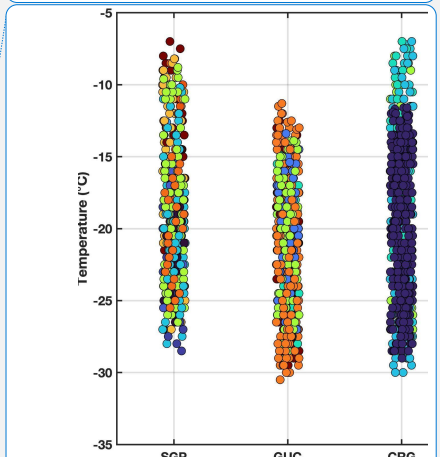

Deleted: ... [1]

In this paper, we focus on the TBS deployments at CRG and BNF where PUFIN was included, and consequently, larger air volumes were collected (Table 1). These conditions produced relatively complete cumulative INP spectra over much shorter collection times (~30 to 60 minutes) compared with previous IcePuck deployments at SGP and GUC, which often required more than an hour to obtain sufficient sample loading for INP detection, given the low flow rate of IcePuck. The shorter collection time is advantageous because it allows sampling at more altitude ranges per flight given constraints on flight duration imposed by battery life and staffing limitations.

At CRG, TBS operations took place in both winter and summer as part of the CoURAGE campaign, which investigates how spatial gradients in land–atmosphere interactions across coastal, urban, and rural environments influence atmospheric processes such as aerosols, clouds, radiation, precipitation, and boundary-layer dynamics in the Baltimore region. A central objective of CoURAGE is to improve representation of coastal urban climates in Earth system models by leveraging

observations from a four-node regional observatory network to test and refine model simulations of urban atmospheric environments. The BNF observatory, a long-term ARM mobile facility (AMF) located in northwest Alabama, United States, is designed to advance understanding of the coupled interactions among aerosols, clouds, and land–atmosphere processes, particularly within forested environments, to strengthen their representation in Earth system models. In addition, BNF is envisioned to serve as a testbed for applying artificial intelligence and machine learning methods to enhance predictability in atmospheric science, while supporting detailed studies of land–atmosphere feedbacks and aerosol–cloud interactions. To date, four TBS deployments have been conducted at BNF during spring and summer, with additional campaigns anticipated in the future.

4.2 INP profile data from recent ARM TBS campaigns

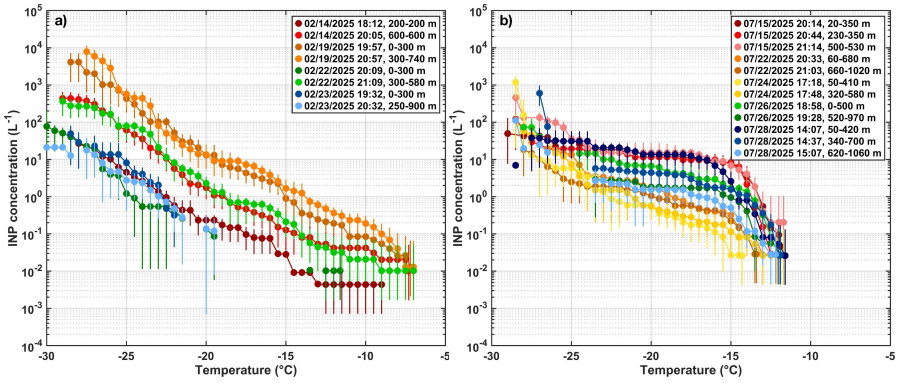

Figure 5: Cumulative INP spectra from CRG TBS flights in a) February and b) July 2025. Two altitudes or altitude ranges were sampled per day. PUFIN loitered at a single altitude if the range is the same value; if a range with different values is listed, PUFIN profiled within that range to collect the sample. Date (mm/dd/yyyy) and time (hh:mm:ss) indicate the sampling (flight) start in UTC. Each day is a different color, with each altitude (range, in m AGL) a different shade of that color. Error bars indicate 95% confidence intervals.

The objective of this section is to provide an initial presentation of the temperature spectra, demonstrating the capabilities of the dataset and highlighting its potential for future scientific investigation. A more in-depth scientific interpretation of these data falls beyond the primary scope of this manuscript; however, we encourage the community to further explore these observations in combination with complementary meteorological and aerosol measurements. Figure 5 shows cumulative INP spectra from CRG during February and July 2025, with darker shades of each color representing the lower altitude sampled each day. We also evaluated equivalent potential temperature (θ_e) during flight days using data collected from the TBS to assess whether the boundary layer in the PUFIN sampling region was well mixed, where INP concentrations would be

Deleted: 6

Formatted: Font: 10 pt

Deleted: Figure 6

Deleted: θ_e

Formatted: Font color: Text 1

Formatted: Font: Italic, Font color: Text 1

Formatted: Font: Italic, Font color: Text 1, Subscript

Formatted: Font color: Text 1

expected to be similar across altitudes, or stratified, which can promote aerosol layering (Creamean et al., 2021; Griesche et al., 2021, 2025). Details of the θ_e calculations are provided in the Supporting Information.

In February, multiple flights were conducted, with two altitudes sampled per day, revealing substantial variability both in overall INP concentrations and in the vertical structure. For example, on 14 and 22 February (red and green shades, respectively), higher altitudes (loitering at 600 m and 300–575 m, respectively) consistently exhibited significant elevated INP concentrations (i.e., spectra varied beyond the 95% confidence intervals) across all temperatures compared with lower altitudes (200 m and 0–300 m, respectively). These days also corresponded to a fairly stratified part of the boundary layer during the flights, since θ_e varied vertically by ~2 to 4 K (Figure S3). In contrast, on 19 and 23 February (orange and blue shades, respectively), no significant differences were observed between upper and lower altitude levels (0–300 m versus 300–740 m and 0–300 m versus 250–900 m, respectively), as concentrations overlapped within the 95% confidence intervals. The boundary layer during the flights appeared to be well mixed on 19 February (θ_e varied by only ~1 K vertically) but stratified on 23 February (Figure S3); therefore, the observed differences in INP spectra are unlikely to be driven solely by distinct aerosol layers. In July, INP concentrations averaged an order of magnitude lower (19 L^{-1}) than in February (145 L^{-1}) at –25 °C, but were an order of magnitude higher at –15 °C (3 versus 0.6 L^{-1}). Interestingly, even the sample collected over just 4 minutes (31 L of air) yielded detectable INP concentrations and was among the higher values observed at CRG at all temperatures. The spectral shapes also differed: February spectra were more log-linear, whereas July spectra exhibited a sharp increase in concentration before –15 °C followed by a plateau, consistent with the influence of biological INPs (Creamean et al., 2019). This is notable given that Baltimore is an urban environment, yet it may still be influenced by biological activity linked to ice nucleation activity, which has been observed in other urban environments (Cabrera-Segoviano et al., 2022; Tobo et al., 2020; Yadav et al., 2019). However, the Baltimore region is bordered by farmland to the east where the dominant crops are grains, oilseeds, dry beans, and dry peas (USDA, 2022), which may have influenced the sampled INP population. Higher freezing temperatures were reached in February due to larger sampling volumes (Table 1), with detection up to –7 °C compared to –11 °C in July. In July, the flights on 22 Jul, 26 Jul, and the lowest (53–423 m) and highest (618–1062 m) altitude ranges on 28 Jul had significant differences. During all three cases, higher INP concentrations were observed at the lower altitude ranges than the upper ranges, which was the opposite of the February observations. These dates also coincided with a stratified vertical structure based on θ_e profiles (Figure S3).

Figure 6, similar to Figure 5, presents results from BNF flights across four months in 2025. In March, INPs were limited to relatively colder temperatures (≤ −14 °C), despite the highest sampled air volumes at BNF compared to other months (Table 1), and no significant differences were observed between altitude levels on any day. The boundary layer during the 27 March flight was highly stratified, but was well mixed on the 21 and 22 March flights (Figure S4). In April, only one day included two altitude levels, which again showed no statistically significant difference. Generally, April exhibited average concentrations comparable to those observed in March (13 and 10 L^{-1} at –25 °C, respectively). By the end of April, a single sample was collected over the full flight from ground level to 850 m, and concentrations began to increase toward the warmer

Deleted: θ_e

Deleted: statistically

Deleted: (two-sample t-test; p < 0.02)

Formatted: Subscript

Deleted: statistically

Deleted: ($p > 0.07$)

Deleted: Warmer

Deleted: statistically

Deleted: (i.e., spectra varied beyond the 95% confidence intervals) ($p = 0.04$, 0.02, and 0.05, respectively)

Formatted: Subscript

Deleted: Figure 7

Deleted: Figure 6

Deleted: In March, INPs were limited to relatively colder temperatures (≤ –14 °C)—even though the highest volumes of air were sampled compared to other months at BNF (Table 1)—and no statistically significant differences were observed between altitude levels on any day ($p > 0.10$).

Deleted: ($p = 0.77$)

end of the spectrum. May involved one flight towards the end of the month at two altitude levels with no difference in INP concentration, likely due to the well-mixed boundary layer (Figure S4), and were similar in concentration to March and April on average (12 L^{-1} at –25 °C). Although the 1 June samples did not show a significant difference, likely due to the generally well-mixed boundary layer aside from a near-surface inversion, the higher altitude range exhibited an order of magnitude higher INP concentration than the lower range (42 versus 4 L^{-1} at –25 °C). Later in June, concentrations increased at higher freezing temperatures, and a significant difference was observed during the 15 June flight, with the lower altitude range showing higher INP concentrations (41 versus 5 L^{-1} at –25 °C), opposite to the pattern observed earlier in the month. Again, this is consistent with the boundary layer structure, which was well mixed on 6 June and stratified on 15 June (Figure S4). The increase towards the end of June suggests that as summer approaches, biological activity in the forest likely intensifies, producing biological INPs active at higher freezing temperatures as evidenced by the spectral shape (Creamean et al., 2019). This is also consistent with observations of increased INPs and bioaerosols during summer in other forested regions (Petersson Sjögren et al., 2023; Schneider et al., 2021; Schumacher et al., 2013). Combined with CRG, these results highlight highly variable vertical and seasonal trends in INP concentrations at a single location, as captured by PUFIN and processed offline with the INS, yielding publicly available data for further exploration by the research community.

At −20 °C, the INP concentrations observed at CRG (0.01–1 L-1 in winter; 0.01–12 L-1 in summer) and BNF (0.01–1 L-1 in spring; 0.02–11 L-1 in summer) fall within the broad range reported in recent studies. For example, Creamean et al. (2018) reported 1–11 L-1 in springtime agricultural regions in Colorado from vertically-resolved filters via a launched and retrieved balloon system, while similar concentrations (~0.02–12 L-1) were observed by Bieber et al. (2020) and Seifried et al. (2021) near a lake in Austria in summer via UAS. Böhmländer et al. (2025) reported lower values of ~0.2–0.5 L-1 during spring and autumn UAS test flights in a boreal environment in Finland. In April in Cyprus, Marinou et al. (2019) reported ~3 L-1 from UAS measurements. Values ranging from ~0.2–10 L-1 from size-resolved measurements have been reported by Porter et al. (2020) across multiple sites in Europe and the Arctic using balloon-based sampling. Overall, the concentrations reported here are consistent with the range of environments sampled in the literature, spanning relatively clean to more biologically or terrestrially influenced regions.

Overall, the flights conducted to date demonstrate that PUFIN can collect sufficient aerosol loadings to capture concentrations as low as 10^{-2} INP L^{-1} in as little as 28 minutes (equivalent to ~250 L of air; 4 minutes at 31 L of air is achievable but at a higher detection limit of 10^{-1} INP L^{-1}). For comparison, INP spectra from SGP and GUC TBS flights are shown in Figures S1 and S2, respectively, in which the same detection limit is achieved but from a longer sampling duration as discussed in Section 4.1. By comparison, ground-based ARM INP measurements are typically collected over 24 hours (~10000 to 30000 L of air), enabling lower detection limits of 10^{-4} INP L^{-1} (Creamean et al., 2025a). Although PUFIN cannot yet achieve such low concentrations, it provides valuable vertically-resolved INP measurements detectable at temperatures as high as –7 °C from measurements thus far. Longer collection durations may further extend detection toward higher

Deleted: statistical
Deleted: (p = 0.42)
Deleted: statistically
Deleted: (p = 0.14)
Deleted: warmer
Deleted: statistically
Deleted: (p = 0.00)
Deleted: is
Deleted: warmer
Deleted: warm
Deleted: warmer

temperatures, potentially above –7 °C. However, further testing in environments with known warm-temperature INPs, such as *Pseudomonas syringae*, is needed to determine whether PUFIN can adequately capture them.

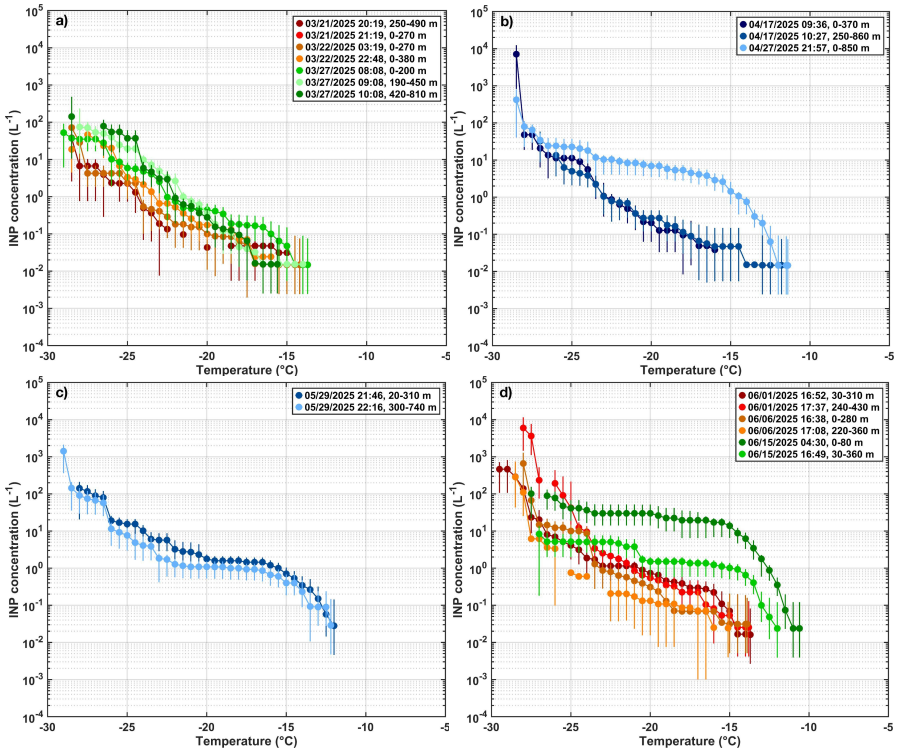

Figure 6: Same as Figure 6, but for BNF in a) March, b) April, c) May, and d) June 2025.

4.3 Requesting PUFIN for future ARM TBS campaigns and beyond

Researchers interested in deploying PUFIN on an ARM TBS mission should first consider contacting the INP and TBS mentors (co-authors of this manuscript, Jessie Creamean and Darielle Dexheimer) to discuss the feasibility, timing, and

Formatted: Justified, Line spacing: 1.5 lines

Deleted: 7

logistical considerations of potential campaigns. Two identical PUFIN units are currently available, including the original system and a newly constructed duplicate. An intercomparison test was conducted using standard ARM ground-based INP filters (Creamean et al., 2025), in which ambient samples were collected outside CSU for 30 minutes, using the first sample valves on both PUFIN systems. The resulting INP spectra show good agreement between the two units, and the ground-based INP filters deployed routinely at ARM sites, demonstrating reproducibility and consistency in sampling and analysis (Figure S5).

Formal requests for PUFIN deployment are submitted through the ARM TBS proposal process, following the guidelines provided on the TBS campaign website (https://www.arm.gov/guidance/campaign-guidelines/tbs). PUFIN is currently configured for deployment on the ARM user facility TBS system, but the design is flexible and could be adapted for use on other balloon platforms or UASs, contingent on community interest. Users may also request sample collection for total INP concentrations, as well as the application of thermal and peroxide treatments to infer INP types, including heat-labile (likely biological), heat-stable (likely organic), and inorganic (likely mineral) INPs (Barry et al., 2023, 2025; DeMott et al., 2025; Hill et al., 2016; McCluskey et al., 2018; Schiebel et al., 2016; Suski et al., 2018; Testa et al., 2021; Tobo et al., 2019). Proposals must target existing ARM observatories, adhere to specific submission deadlines, and include sufficient detail on desired sampling locations, altitudes, and measurement objectives. Both ARM-only and collaborative campaigns are supported. For example, researchers may propose joint ARM–EMSL FICUS (Facilities Integrating Collaborations for User Science) missions to deploy guest instruments, leverage specialized laboratory capabilities, and access additional resources to enhance the scientific output of the campaign (https://www.emsl.pnnl.gov/proposals/type/ficus-program). Detailed information on proposal requirements, timelines, and eligible instruments is provided on the ARM TBS guidance webpage.

5 Summary

This paper introduces PUFIN (Profiling Upper altitudes For Ice Nucleation), a robust INP sampling system developed for routine deployment on the DOE ARM TBS platform. INPs, though present at concentrations orders of magnitude lower than CCN, exert a strong influence on cloud microphysics, lifetime, and radiative properties, particularly in mixed-phase clouds. Accurate representation of INPs in weather and climate models requires knowledge of their vertical distribution, which is often not captured by surface-based measurements or short-duration crewed aircraft observations. Small, flexible platforms such as TBS allow multi-hour, vertically-resolved sampling at targeted altitudes below, within, and above clouds.

PUFIN collects filters at up to three altitudes plus a field blank per flight, and all operations are fully ground-controlled. The collected samples are processed offline using the INS at Colorado State University, producing cumulative INP spectra across subzero temperatures. Recent deployments in Baltimore, Maryland (CRG) and Bankhead National Forest, Alabama (BNF) demonstrate that PUFIN can detect INP concentrations as low as ~10^{-3} L^{-1} in as little as 28 minutes, a substantial improvement over the older ARM TBS INP sampling system and enabling multiple altitude profiles per flight. CRG data revealed notable

vertical variability in INP concentrations likely linked to boundary layer stratification and aerosol transport, while BNF exhibited generally lower INP concentrations with limited vertical dependence. All PUFIN-generated INP data are publicly available via the ARM Data Center, and researchers can request PUFIN deployment for future TBS campaigns, including collaborative missions at existing and future proposed ARM observatories.

As PUFIN has only been deployed a limited number of times to date, we are still actively identifying best practices. While we have not yet fully evaluated performance under extreme environmental conditions, future deployments will require careful consideration of such factors. Initial experience highlights the importance of maximizing sampling volume for robust INP detection and the value of sending test samples from new or unfamiliar environments for immediate analysis to inform subsequent sampling strategies. We also note that inlet components (e.g., hose barbs) may introduce minor collection efficiency losses, though further testing is needed to assess potential trade-offs with background contamination during ascent and descent. Maintaining consistent altitude ranges where possible improves comparability, and future dedicated flights are planned to include longer-duration sampling at fixed "loitering" altitudes to better resolve vertical structure and potentially achieve even lower detection limits.

Future improvements to PUFIN will focus on enhancing altitude accuracy, overall system robustness, and evaluating particle removal methodologies to ensure the most effective approach is used. Planned upgrades include the incorporation of pressure-based altitude measurements and higher-accuracy GPS sensors, as well as standardized reporting of altitude relative to surface elevation (AGL) to facilitate inter-site comparisons. In addition, improvements to power management, particularly more reliable charging and distribution for onboard sensors, are anticipated to ensure stable operation during extended deployments. For particle removal from the filters, this approach has been intercompared with other techniques employing different extraction methods and showed good agreement (DeMott et al., 2017, 2025; Lasher et al., 2024). Future work will evaluate a range of rotation times to ensure that the current 20-minute extraction is sufficient across filters with varying particle loadings.

Looking forward, expanding the use of PUFIN and similar systems as TBS operations become more routine would not only provide more comprehensive assessments of vertical INP distributions but also capture seasonal variability in these profiles. By providing high-resolution, vertically-stratified INP measurements, PUFIN enhances understanding of aerosol-cloud interactions, informs representation of INPs in models, and supports studies of regional to global climate processes.

Data availability

TBSINP data are available from the DOE ARM Data Center (https://www.arm.gov/data) or Data Discovery portal (https://adc.arm.gov/discovery/) under DOI https//doi.org/10.5439/2001041 (Creamean et al., 2024). PUFIN design drawing and parts list are available at https://github.com/ARM-Development/TBS-INP-Design.

Author contributions

JMC and AT conceptualised the INP mentor program. JMC, CCH, DD, and BTMH designed the TBSINP sampler, while BTMH built it. DD, CL, and CR were responsible for TBS deployments at ARM sites. CCH and MV conducted the sample and data analysis for the TBSINP data that are publicly-available for download from the DOE ARM Data Center. All authors contributed to the writing of this manuscript.

Competing interests

None of the authors has any competing interests.

Disclaimer

Publisher's note: Copernicus Publications remains neutral with regard to jurisdictional claims made in the text, published maps, institutional affiliations, or any other geographical representation in this paper. While Copernicus Publications makes every effort to include appropriate place names, the final responsibility lies with the authors.

Acknowledgements

This work was supported by the Office of Biological and Environmental Research within the U.S. Department of Energy (DOE) through the Atmospheric Radiation Measurement (ARM) user facility. JMC, CCH, and MV received support under DOE contract no. DE-0F-60173. We gratefully acknowledge James Mather for his invaluable support in the development and implementation of the INP program. We also extend our sincere thanks to the ARM site staff for their significant assistance with instrument installation, sample collection, and logistics. We gratefully acknowledge Thomas C. J. Hill for his foundational role as co-mentor alongside JMC during the inception of this program, and for his enduring guidance and expertise. He is now enjoying a well-earned retirement in Australia. ChatGPT was used to assist in editing and improving the wording of this manuscript.

Financial support

This research has been supported by Argonne National Laboratory for the DOE under contract DE-0F-60173.

References

Agresti, A. and Coull, B. A.: Approximate Is Better than “Exact” for Interval Estimation of Binomial Proportions, Am. Stat., 52, 119, https://doi.org/10.2307/2685469, 1998.

Barry, K. R., Hill, T. C. J., Jentzsch, C., Moffett, B. F., Stratmann, F., and DeMott, P. J.: Pragmatic protocols for working cleanly when measuring ice nucleating particles, Atmospheric Res., 250, 105419, https://doi.org/10.1016/j.atmosres.2020.105419, 2021.

Barry, K. R., Hill, T. C. J., Nieto-Caballero, M., Douglas, T. A., Kreidenweis, S. M., DeMott, P. J., and Creamean, J. M.: Active thermokarst regions contain rich sources of ice nucleating particles, EGUsphere, 1–19, https://doi.org/10.5194/egusphere-2023-1208, 2023.

Barry, K. R., Hill, T. C. J., Kreidenweis, S. M., DeMott, P. J., Tobo, Y., and Creamean, J. M.: Bioaerosols as indicators of central Arctic ice nucleating particle sources, Atmospheric Chemistry and Physics, 25, 11919–11933, https://doi.org/10.5194/acp-25-11919-2025, 2025.

Beall, C. M., Stokes, M. D., Hill, T. C., DeMott, P. J., DeWald, J. T., and Prather, K. A.: Automation and heat transfer characterization of immersion mode spectroscopy for analysis of ice nucleating particles, Atmospheric Meas. Tech., 10, 2613–2626, https://doi.org/10.5194/amt-10-2613-2017, 2017.

Beall, C. M., Lucero, D., Hill, T. C., DeMott, P. J., Stokes, M. D., and Prather, K. A.: Best practices for precipitation sample storage for offline studies of ice nucleation in marine and coastal environments, Atmos. Meas. Tech., 13, 6473–6486, https://doi.org/10.5194/amt-13-6473-2020, 2020.

Bieber, P., Seifried, T. M., Burkart, J., Gratzl, J., Kasper-Giebl, A., Schmale, D. G., and Grothe, H.: A Drone-Based Bioaerosol Sampling System to Monitor Ice Nucleation Particles in the Lower Atmosphere, Remote Sensing, 12, 552, https://doi.org/10.3390/rs12030552, 2020.

Böhmländer, A., Lacher, L., Brus, D., Doulgeris, K.-M., Brasseur, Z., Boyer, M., Kuula, J., Leisner, T., and Möhler, O.: A novel aerosol filter sampler for measuring the vertical distribution of ice-nucleating particles via fixed-wing uncrewed aerial vehicles, Atmospheric Meas. Tech., 18, 3959–3971, https://doi.org/10.5194/amt-18-3959-2025, 2025.

Burrows, S. M., McCluskey, C. S., Cornwell, G., Steinke, I., Zhang, K., Zhao, B., Zawadowicz, M., Raman, A., Kulkarni, G., China, S., Zelenyuk, A., and DeMott, P. J.: Ice-Nucleating Particles That Impact Clouds and Climate: Observational and Modeling Research Needs, Rev. Geophys., 60, e2021RG000745, https://doi.org/10.1029/2021RG000745, 2022.

Cabrera-Segoviano, D., Pereira, D. L., Rodriguez, C., Raga, G. B., Miranda, J., Alvarez-Ospina, H., and Ladino, L. A.: Inter-annual variability of ice nucleating particles in Mexico city, Atmos. Environ., 273, 118964, https://doi.org/10.1016/j.atmosenv.2022.118964, 2022.

Chatziparaschos, M., Myriokefalitakis, S., Kalivitis, N., Daskalakis, N., Nenes, A., Gonçalves Ageitos, M., Costa-Surós, M., Pérez García-Pando, C., Vrekoussis, M., and Kanakidou, M.: Assessing the global contribution of marine aerosols, terrestrial bioaerosols, and desert dust to ice-nucleating particle concentrations, Atmospheric Chem. Phys., 25, 9085–9111, https://doi.org/10.5194/acp-25-9085-2025, 2025.

Cornwell, G. C., Steinke, I., Lata, N. N., Zelenyuk, A., Kulkarni, G., Pekour, M., Perkins, R., Levin, E. J. T., China, S., DeMott, P. J., and Burrows, S. M.: Enrichment of Phosphates, Lead, and Mixed Soil-Organic Particles in INPs at the Southern Great Plains Site, J. Geophys. Res. Atmospheres, 129, e2024JD040826, https://doi.org/10.1029/2024JD040826, 2024.

Creamean, J., Hill, T., Hume, C., and Devadoss, T.: Ice Nucleation Spectrometer (INS) Instrument Handbook, U.S. Department of Energy, Atmospheric Radiation Measurement user facility, Richland, Washington, 2024.

Creamean, J. M., Primm, K. M., Tolbert, M. A., Hall, E. G., Wendell, J., Jordan, A., Sheridan, P. J., Smith, J., and Schnell, R. C.: HOVERCAT: a novel aerial system for evaluation of aerosol–cloud interactions, Atmospheric Meas. Tech., 11, 3969–3985, https://doi.org/10.5194/amt-11-3969-2018, 2018.

Creamean, J. M., Mignani, C., Bukowiecki, N., and Conen, F.: Using freezing spectra characteristics to identify ice-nucleating particle populations during the winter in the Alps, Atmospheric Chem. Phys., 19, 8123–8140, https://doi.org/10.5194/acp-19-8123-2019, 2019.

Creamean, J. M., de Boer, G., Telg, H., Mei, F., Dexheimer, D., Shupe, M. D., Solomon, A., and McComiskey, A.: Assessing the vertical structure of Arctic aerosols using balloon-borne measurements, Atmospheric Chem. Phys., 21, 1737–1757, https://doi.org/10.5194/acp-21-1737-2021, 2021.

Creamean, J. M., Hume, C. C., Vazquez, M., and Theisen, A.: Long-term measurements of ice nucleating particles at Atmospheric Radiation Measurement (ARM) sites worldwide, Earth Syst. Sci. Data Discuss., 1–31, https://doi.org/10.5194/essd-2025-352, 2025a.

Creamean, J. M., L. A. Miller, M. van Pinxteren, O. Crabeck, N. S. Steiner, L. Marelle, I. Deschepper, R. Lapere, A. Leon-Marcos, K. A. Pratt, J. L. Thomas, A. Da Silva, M. M. Frey, I. Peeken, H. Horowitz, M. D. Willis, and R. Price: Polar primary aerosols across the ocean-sea ice-snow-atmosphere interface: from sources to impacts, Elem. Sci. Anthr., in revision, 2025b.

DeMott, P. J., Hill, T. C. J., Petters, M. D., Bertram, A. K., Tobo, Y., Mason, R. H., Suski, K. J., McCluskey, C. S., Levin, E. J. T., Schill, G. P., Boose, Y., Rauker, A. M., Miller, A. J., Zaragoza, J., Rocci, K., Rothfuss, N. E., Taylor, H. P., Hader, J. D., Chou, C., Huffman, J. A., Pöschl, U., Prenni, A. J., and Kreidenweis, S. M.: Comparative measurements of ambient atmospheric concentrations of ice nucleating particles using multiple immersion freezing methods and a continuous flow diffusion chamber, Atmospheric Chem. Phys., 17, 11227–11245, https://doi.org/10.5194/acp-17-11227-2017, 2017.

DeMott, P. J., Mirrielees, J. A., Petters, S. S., Cziczo, D. J., Petters, M. D., Bingemer, H. G., Hill, T. C. J., Froyd, K., Garimella, S., Hallar, A. G., Levin, E. J. T., McCubbin, I. B., Perring, A. E., Rapp, C. N., Schiebel, T., Schrod, J., Suski, K. J., Weber, D., Wolf, M. J., Zawadowicz, M., Zenker, J., Möhler, O., and Brooks, S. D.: Field intercomparison of ice nucleation measurements: the Fifth International Workshop on Ice Nucleation Phase 3 (FIN-03), Atmospheric Measurement Techniques, 18, 639–672, https://doi.org/10.5194/amt-18-639-2025, 2025.

Dexheimer, D., Whitson, G., Cheng, Z., Sammon, J., Gaustad, K., Mei, F., and Longbottom, C.: Tethered Balloon System (TBS) Instrument Handbook, https://doi.org/10.2172/1415858, 2024.

Feldman, D. R., Aiken, A. C., Boos, W. R., Carroll, R. W. H., Chandrasekar, V., Collis, S., Creamean, J. M., Boer, G. de, Deems, J., DeMott, P. J., Fan, J., Flores, A. N., Gochis, D., Grover, M., Hill, T. C. J., Hodshire, A., Hulm, E., Hume, C. C., Jackson, R., Junyent, F., Kennedy, A., Kumjian, M., Levin, E. J. T., Lundquist, J. D., O'Brien, J., Raleigh, M. S., Reithel, J., Rhoades, A., Rittger, K., Rudisill, W., Sherman, Z., Siirila-Woodburn, E., Skiles, S. M., Smith, J. N., Sullivan, R. C., Theisen, A., Tuftedal, M., Varble, A. C., Wiedlea, A., Wielandt, S., Williams, K., and Xu, Z.: The Surface Atmosphere Integrated Field Laboratory (SAIL) Campaign, https://doi.org/10.1175/BAMS-D-22-0049.1, 2023.

Griesche, H. J., Ohneiser, K., Seifert, P., Radenz, M., Engelmann, R., and Ansmann, A.: Contrasting ice formation in Arctic clouds: surface-coupled vs. surface-decoupled clouds, Atmospheric Chem. Phys., 21, 10357–10374, https://doi.org/10.5194/acp-21-10357-2021, 2021.

Griesche, H. J., Engelmann, R., Radenz, M., Hofer, J., Althausen, D., Ansmann, A., Barry, K., Creamean, J., Jimenez, C., and Seifert, P.: Annual cycle of surface-coupling effects on Arctic mixed-phase clouds during MOSAiC, EGUsphere, 1–33, https://doi.org/10.5194/egusphere-2025-5708, 2025.

Guy, H., Martin, A. S., Olson, E., Brooks, I. M., and Neely III, R. R.: Measurement report: In situ vertical profiles of below-cloud aerosol over the central Greenland Ice Sheet, Atmospheric Chem. Phys., 24, 11103–11114, https://doi.org/10.5194/acp-24-11103-2024, 2024.

Hill, T. C. J., DeMott, P. J., Tobo, Y., Fröhlich-Nowoisky, J., Moffett, B. F., Franc, G. D., and Kreidenweis, S. M.: Sources of organic ice nucleating particles in soils, Atmospheric Chem. Phys., 16, 7195–7211, https://doi.org/10.5194/acp-16-7195-2016, 2016.

Hiranuma, N., Augustin-Bauditz, S., Bingemer, H., Budke, C., Curtius, J., Danielczok, A., Diehl, K., Dreischmeier, K., Ebert, M., Frank, F., Hoffmann, N., Kandler, K., Kiselev, A., Koop, T., Leisner, T., Möhler, O., Nillius, B., Peckhaus, A., Rose, D., Weinbruch, S., Wex, H., Boose, Y., DeMott, P. J., Hader, J. D., Hill, T. C. J., Kanji, Z. A., Kulkarni, G., Levin, E. J. T., McCluskey, C. S., Murakami, M., Murray, B. J., Niedermeier, D., Petters, M. D., O'Sullivan, D., Saito, A., Schill, G. P., Tajiri, T., Tolbert, M. A., Welti, A., Whale, T. F., Wright, T. P., and Yamashita, K.: A comprehensive laboratory study on the immersion freezing behavior of illite NX particles: a comparison of 17 ice nucleation measurement techniques, Atmospheric Chem. Phys., 15, 2489–2518, https://doi.org/10.5194/acp-15-2489-2015, 2015.

Kanji, Z. A., Ladino, L. A., Wex, H., Boose, Y., Burkert-Kohn, M., Cziczo, D. J., and Krämer, M.: Overview of ice nucleating particles, Meteor Monogr, 58, 1.1-1.33, https://doi.org/10.1175/AMSMONOGRAPHS-D-16-0006.1, 2017.

Knopf, D. A., Barry, K. R., Brubaker, T. A., Jahl, L. G., Jankowski, K. A., Li, J., Lu, Y., Monroe, L. W., Moore, K. A., Rivera-Adorno, F. A., Sauceda, K. A., Shi, Y., Tomlin, J. M., Vepuri, H. S. K., Wang, P., Lata, N. N., Levin, E. J. T., Creamean, J. M., Hill, T. C. J., China, S., Alpert, P. A., Moffet, R. C., Hiranuma, N., Sullivan, R. C., Fridlind, A. M., West, M., Riemer, N., Laskin, A., DeMott, P. J., and Liu, X.: Aerosol–Ice Formation Closure: A Southern Great Plains Field Campaign, Bull. Am. Meteorol. Soc., 102, E1952–E1971, https://doi.org/10.1175/BAMS-D-20-0151.1, 2021.

Lacher, L., Adams, M. P., Barry, K., Bertozzi, B., Bingemer, H., Boffo, C., Bras, Y., Büttner, N., Castarede, D., Cziczo, D. J., DeMott, P. J., Fösig, R., Goodell, M., Höhler, K., Hill, T. C. J., Jentzsch, C., Ladino, L. A., Levin, E. J. T., Mertes, S., Möhler, O., Moore, K. A., Murray, B. J., Nadolny, J., Pfeuffer, T., Picard, D., Ramírez-Romero, C., Ribeiro, M., Richter, S., Schrod, J., Sellegri, K., Stratmann, F., Swanson, B. E., Thomson, E. S., Wex, H., Wolf, M. J., and Freney, E.: The Puy de Dôme ICe Nucleation Intercomparison Campaign (PICNIC): comparison between online and offline methods in ambient air, Atmospheric Chem. Phys., 24, 2651–2678, https://doi.org/10.5194/acp-24-2651-2024, 2024.

Marinou, E., Tesche, M., Nenes, A., Ansmann, A., Schrod, J., Mamali, D., Tsekeri, A., Pikridas, M., Baars, H., Engelmann, R., Voudouri, K.-A., Solomos, S., Sciare, J., Groß, S., Ewald, F., and Amiridis, V.: Retrieval of ice-nucleating particle concentrations from lidar observations and comparison with UAV in situ measurements, Atmos. Chem. Phys., 19, 11315–11342, https://doi.org/10.5194/acp-19-11315-2019, 2019.

Lonardi, M., Pilz, C., Akansu, E. F., Dahlke, S., Egerer, U., Ehrlich, A., Griesche, H., Heymsfield, A. J., Kirbus, B., Schmitt, C. G., Shupe, M. D., Siebert, H., Wehner, B., and Wendisch, M.: Tethered balloon-borne profile measurements of atmospheric properties in the cloudy atmospheric boundary layer over the Arctic sea ice during MOSAiC: Overview and first results, Elem. Sci. Anthr., 10, 000120, https://doi.org/10.1525/elementa.2021.000120, 2022.

McCluskey, C. S., Hill, T. C. J., Malfatti, F., Sultana, C. M., Lee, C., Santander, M. V., Beall, C. M., Moore, K. A., Cornwell, G. C., Collins, D. B., Prather, K. A., Jayarathne, T., Stone, E. A., Azam, F., Kreidenweis, S. M., and DeMott, P. J.: A Dynamic Link between Ice Nucleating Particles Released in Nascent Sea Spray Aerosol and Oceanic Biological Activity during Two Mesocosm Experiments, J. Atmospheric Sci., 74, 151–166, https://doi.org/10.1175/JAS-D-16-0087.1, 2017.

McCluskey, C. S., Hill, T. C. J., Humphries, R. S., Rauker, A. M., Moreau, S., Strutton, P. G., Chambers, S. D., Williams, A. G., McRobert, I., Ward, J., Keywood, M. D., Harnwell, J., Ponsonby, W., Loh, Z. M., Krummel, P. B., Protat, A.,

669 Kreidenweis, S. M., and DeMott, P. J.: Observations of ice nucleating particles over Southern Ocean waters, Geophysical
670 Research Letters, 45, 11,989-11,997, https://doi.org/10.1029/2018GL079981, 2018.

671 Mei, F., Zhang, Q., Zhang, D., Fast, J. D., Kulkarni, G., Pekour, M. S., Niedek, C. R., Glienke, S., Silber, I., Schmid, B.,
672 Tomlinson, J. M., Mehta, H. S., Mansoura, X., Cheng, Z., Vandergrift, G. W., Lata, N. N., China, S., and Zhu, Z.:
673 Measurement report: Vertically resolved atmospheric properties observed over the Southern Great Plains with the
674 ArcticShark uncrewed aerial system, Atmospheric Chem. Phys., 25, 3425–3444, https://doi.org/10.5194/acp-25-3425-2025,
675 2025.

676 Mülmenstädt, J., Sourdeval, O., Delanoë, J., and Quaas, J.: Frequency of occurrence of rain from liquid-, mixed-, and ice-
677 phase clouds derived from A-Train satellite retrievals: RAIN FROM LIQUID- AND ICE-PHASE CLOUDS, Geophys. Res.
678 Lett., 42, 6502–6509, https://doi.org/10.1002/2015GL064604, 2015.

679 Murray, B. J., Carslaw, K. S., and Field, P. R.: Opinion: Cloud-phase climate feedback and the importance of ice-nucleating
680 particles, Atmospheric Chem. Phys., 21, 665–679, https://doi.org/10.5194/acp-21-665-2021, 2021.

681 Petersson Sjögren, M., Alsved, M., Šantl-Temkiv, T., Bjerring Kristensen, T., and Löndahl, J.: Measurement report:
682 Atmospheric fluorescent bioaerosol concentrations measured during 18 months in a coniferous forest in the south of Sweden,
683 Atmospheric Chem. Phys., 23, 4977–4992, https://doi.org/10.5194/acp-23-4977-2023, 2023.

684 Pilz, C., Düsing, S., Wehner, B., Müller, T., Siebert, H., Voigtländer, J., and Lonardi, M.: CAMP: an instrumented platform
685 for balloon-borne aerosol particle studies in the lower atmosphere, Atmospheric Meas. Tech., 15, 6889–6905,
686 https://doi.org/10.5194/amt-15-6889-2022, 2022.

687 Pilz, C., Lonardi, M., Egerer, U., Siebert, H., Ehrlich, A., Heymsfield, A. J., Schmitt, C. G., Shupe, M. D., Wehner, B., and
688 Wendisch, M.: Profile observations of the Arctic atmospheric boundary layer with the BELUGA tethered balloon during
689 MOSAiC, Sci. Data, 10, 534, https://doi.org/10.1038/s41597-023-02423-5, 2023.

690 Pilz, C., Cassano, J. J., de Boer, G., Kirbus, B., Lonardi, M., Pöhlker, M., Shupe, M. D., Siebert, H., Wendisch, M., and
691 Wehner, B.: Tethered balloon measurements reveal enhanced aerosol occurrence aloft interacting with Arctic low-level
692 clouds, Elem. Sci. Anthr., 12, 00120, https://doi.org/10.1525/elementa.2023.00120, 2024.

693 Pohorsky, R., Baccarini, A., Tolu, J., Winkel, L. H. E., and Schmale, J.: Modular Multiplatform Compatible Air
694 Measurement System (MoMuCAMS): a new modular platform for boundary layer aerosol and trace gas vertical
695 measurements in extreme environments, Atmospheric Meas. Tech., 17, 731–754, https://doi.org/10.5194/amt-17-731-2024,
696 2024.

697 Pohorsky, R., Baccarini, A., Brett, N., Barret, B., Bekki, S., Pappaccogli, G., Dieudonné, E., Temime-Roussel, B., D'Anna,
698 B., Cesler-Maloney, M., Donateo, A., Decesari, S., Law, K. S., Simpson, W. R., Fochesatto, J., Arnold, S. R., and Schmale,
699 J.: In situ vertical observations of the layered structure of air pollution in a continental high-latitude urban boundary layer
700 during winter, Atmospheric Chem. Phys., 25, 3687–3715, https://doi.org/10.5194/acp-25-3687-2025, 2025.

701 Porter, G. C. E., Sikora, S. N. F., Adams, M. P., Proske, U., Harrison, A. D., Tarn, M. D., Brooks, I. M., and Murray, B. J.:
702 Resolving the size of ice-nucleating particles with a balloon deployable aerosol sampler: the SHARK, Atmospheric Meas.
703 Tech., 13, 2905–2921, https://doi.org/10.5194/amt-13-2905-2020, 2020.

704 Porter, G. C. E., Adams, M. P., Brooks, I. M., Ickes, L., Karlsson, L., Leck, C., Salter, M. E., Schmale, J., Siegel, K., Sikora,
705 S. N. F., Tarn, M. D., Vüllers, J., Wernli, H., Zieger, P., Zinke, J., and Murray, B. J.: Highly active ice-nucleating particles
706 at the summer North Pole, J. Geophys. Res. Atmospheres, 127, e2021JD036059, https://doi.org/10.1029/2021JD036059,
707 2022.

Pruppacher, H. R. and Klett, J. D.: Microphysics of Clouds and Precipitation, Springer Netherlands, Dordrecht, https://doi.org/10.1007/978-0-306-48100-0, 2010.

Schiebel, T., Höhler, K., Funk, R., Hill, T. C. J., Levin, E. J. T., Nadolny, J., Steinke, I., Suski, K. J., Ullrich, R., Wagner, R., Weber, I., DeMott, P. J., and Möhler, O.: Ice nucleation activity of various agricultural soil dust aerosol particles, European Geosciences Union General Assembly, Wien, A, April 17-22, 2016. Geophysical Research Abstracts, 18(2016) EGU2016-13422, 2016.

Seifried, T. M., Bieber, P., Kunert, A. T., Iii, D. G. S., Whitmore, K., Fröhlich-Nowoisky, J., and Grothe, H.: Ice Nucleation Activity of Alpine Bioaerosol Emitted in Vicinity of a Birch Forest, Atmosphere, 12, https://doi.org/10.3390/atmos12060779, 2021.

Schneider, J., Höhler, K., Heikkilä, P., Keskinen, J., Bertozzi, B., Bogert, P., Schorr, T., Umo, N. S., Vogel, F., Brasseur, Z., Wu, Y., Hakala, S., Duplissy, J., Moisseev, D., Kulmala, M., Adams, M. P., Murray, B. J., Korhonen, K., Hao, L., Thomson, E. S., Castarède, D., Leisner, T., Petäjä, T., and Möhler, O.: The seasonal cycle of ice-nucleating particles linked to the abundance of biogenic aerosol in boreal forests, Atmospheric Chem. Phys., 21, 3899–3918, https://doi.org/10.5194/acp-21-3899-2021, 2021.

Schnell, R. C. and Vali, G.: Biogenic Ice Nuclei: Part I. Terrestrial and Marine Sources, J. Atmospheric Sci., 33, 1554–1564, https://doi.org/10.1175/1520-0469(1976)033%253C1554:BINPIT%253E2.0.CO;2, 1976.

Schumacher, C. J., Pöhlker, C., Aalto, P., Hiltunen, V., Petäjä, T., Kulmala, M., Pöschl, U., and Huffman, J. A.: Seasonal cycles of fluorescent biological aerosol particles in boreal and semi-arid forests of Finland and Colorado, Atmospheric Chem. Phys., 13, 11987–12001, https://doi.org/10.5194/acp-13-11987-2013, 2013.

Spurny, K. R. and Lodge, J. P.: Collection Efficiency Tables for Membrane Filters Used in the Sampling and Analysis of Aerosols and Hydrosols, Laboratory of Atmospheric Science, National Center for Atmospheric Research, 56 pp., 1972.

Steiner, A. L.: Role of the Terrestrial Biosphere in Atmospheric Chemistry and Climate, Acc. Chem. Res., 53, 1260–1268, https://doi.org/10.1021/acs.accounts.0c00116, 2020.

Storelvmo, T.: Aerosol Effects on Climate via Mixed-Phase and Ice Clouds, Annu. Rev. Earth Planet. Sci., 45, 199–222, https://doi.org/10.1146/annurev-earth-060115-012240, 2017.

Suski, K. J., Hill, T. C. J., Levin, E. J. T., Miller, A., DeMott, P. J., and Kreidenweis, S. M.: Agricultural harvesting emissions of ice-nucleating particles, Atmospheric Chem. Phys., 18, 13755–13771, https://doi.org/10.5194/acp-18-13755-2018, 2018.

Testa, B., Hill, T. C. J., Marsden, N. A., Barry, K. R., Hume, C. C., Bian, Q., Uetake, J., Hare, H., Perkins, R. J., Möhler, O., Kreidenweis, S. M., and DeMott, P. J.: Ice Nucleating Particle Connections to Regional Argentinian Land Surface Emissions and Weather During the Cloud, Aerosol, and Complex Terrain Interactions Experiment, JGR Atmospheres, 126, https://doi.org/10.1029/2021JD035186, 2021.

Tobo, Y., Adachi, K., DeMott, P. J., Hill, T. C. J., Hamilton, D. S., Mahowald, N. M., Nagatsuka, N., Ohata, S., Uetake, J., Kondo, Y., and Koike, M.: Glacially sourced dust as a potentially significant source of ice nucleating particles, Nat. Geosci., 12, 253–258, https://doi.org/10.1038/s41561-019-0314-x, 2019.

Tobo, Y., Uetake, J., Matsui, H., Moteki, N., Uji, Y., Iwamoto, Y., Miura, K., and Misumi, R.: Seasonal Trends of Atmospheric Ice Nucleating Particles Over Tokyo, J. Geophys. Res. Atmospheres, 125, e2020JD033658, https://doi.org/10.1029/2020JD033658, 2020.

Vali, G.: Quantitative Evaluation of Experimental Results an the Heterogeneous Freezing Nucleation of Supercooled Liquids, J. Atmospheric Sci., 28, 402–409, https://doi.org/10.1175/1520-0469(1971)028%253C0402:QEOERA%253E2.0.CO;2, 1971.

Yadav, S., Venezia, R. E., Paerl, R. W., and Petters, M. D.: Characterization of Ice-Nucleating Particles Over Northern India, J. Geophys. Res. Atmospheres, 124, 10467–10482, https://doi.org/10.1029/2019JD030702, 2019.

Zinke, J., Salter, M. E., Leck, C., Lawler, M. J., Porter, G. C. E., Adams, M. P., Brooks, I. M., Murray, B. J., and Zieger, P.: The development of a miniaturised balloon-borne cloud water sampler and its first deployment in the high Arctic, Tellus B Chem. Phys. Meteorol., 73, 1915614, https://doi.org/10.1080/16000889.2021.1915614, 2021.

Page 12: [1] Deleted **Jessie Creamean** **4/6/26 7:41:00 PM**

Supporting Information

Reaching new heights: Profiling Upper altitudes for Ice Nucleation (PUFIN) on the Atmospheric Radiation Measurement (ARM) tethered balloon systems

Deleted: A vertically-resolved ice nucleating particle sampler operating

Jessie M. Creamean[1], Darielle Dexheimer[2], Carson C. Hume[1], Maria Vazquez[1], Benjamin T. M. Hess[2], Casey M. Longbottom[2], Carlos A. Ruiz[2], Adam K. Theisen[3]

[1]Department of Atmospheric Science, Colorado State University, Fort Collins, Colorado, 80523, USA

[2]Sandia National Laboratory, Albuquerque, New Mexico, 87123, USA

[3]Argonne National Laboratory, Lemont, Illinois, 60439, USA

Correspondence to: Jessie M. Creamean (jessie.creamean@colostate.edu)

Supporting methods

Equivalent potential temperature calculations

Because the iMet-XQ2 accuracy is limited (see Summary section), we use the more reliable TBSIMET observations to examine equivalent potential temperature (θe), calculated following Bolton (1980), which is well suited for assessing atmospheric stratification and boundary-layer mixing. Additionally, for the CRG February flights the iMet-XQ2 data were not recorded in the INP flight data files, although iMet-XQ2 measurements were taken for the July flights. TBSIMET data are available from the ARM Data Center (https://adc.arm.gov/discovery/results/s::tbsimet).

To calculate θe, TBSIMET data (altitude, temperature, pressure, relative humidity) were first preprocessed by removing unrealistic, non-NaN spikes in altitude observations and converting altitude from kilometers to meters. The profiles were then averaged into 10-m vertical bins; within each bin the mean altitude, temperature (°C), pressure (hPa), and relative humidity (%) were computed. Dew point temperature (T_d) in each bin was estimated from the binned temperature and relative humidity using the Magnus–Tetens approximation. Saturation vapor pressure at T_d was computed and the mixing ratio r (kg kg^{-1}) obtained via $r = \varepsilon e_s/(p - e_s)$ with $\varepsilon = 0.622$. Potential temperature θ was calculated from the binned temperature and pressure, and equivalent potential temperature was computed using the Bolton (1980) formulation: $\theta e = \theta \exp((L_v r)/(c_p T_d(K)))$, where L_v is latent heat of vaporization ($\approx 2.5\times10^6$ J kg^{-1}), c_p is the dry-air specific heat at constant pressure ($\approx$1005.7 J kg^{-1} K^{-1}), and $T_d(K)$ is T_d in kelvin. Uncertainty in θ_e was estimated as the one-standard-deviation of θ_e values computed for each original sample within a bin (i.e., compute θ_e per sample, then take the binwise standard deviation).

To determine whether the boundary layer at the PUFIN sampling altitudes was well mixed or stratified, we evaluated θ_e only within the altitude ranges where PUFIN was deployed. If the vertical variation (minimum to maximum) in θ_e was ≤ 1 K, the layer was considered well mixed; if > 1 K, it was classified as stratified. Variability in θ_e could manifest as discrete layers or as a continuous vertical gradient.

Bolton, D.: The Computation of Equivalent Potential Temperature, Mon. Wea. Rev., 108, 1046–1053, https://doi.org/10.1175/1520-0493(1980)108%3C1046:TCOEPT%3E2.0.CO;2, 1980.

Formatted: Font: Italic

Formatted ... [1]

Formatted ... [2]

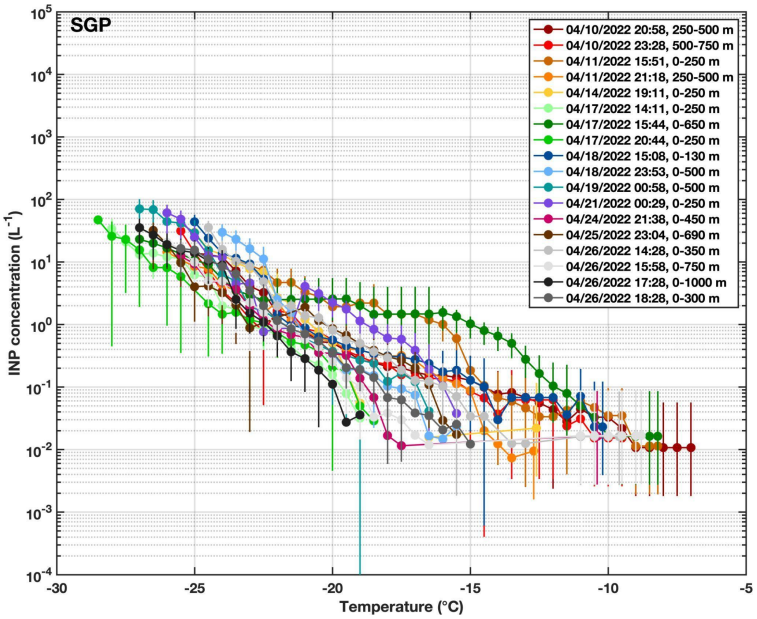

Figure S1. Same as Figure 5, but for SGP in April 2022.

Deleted: 6

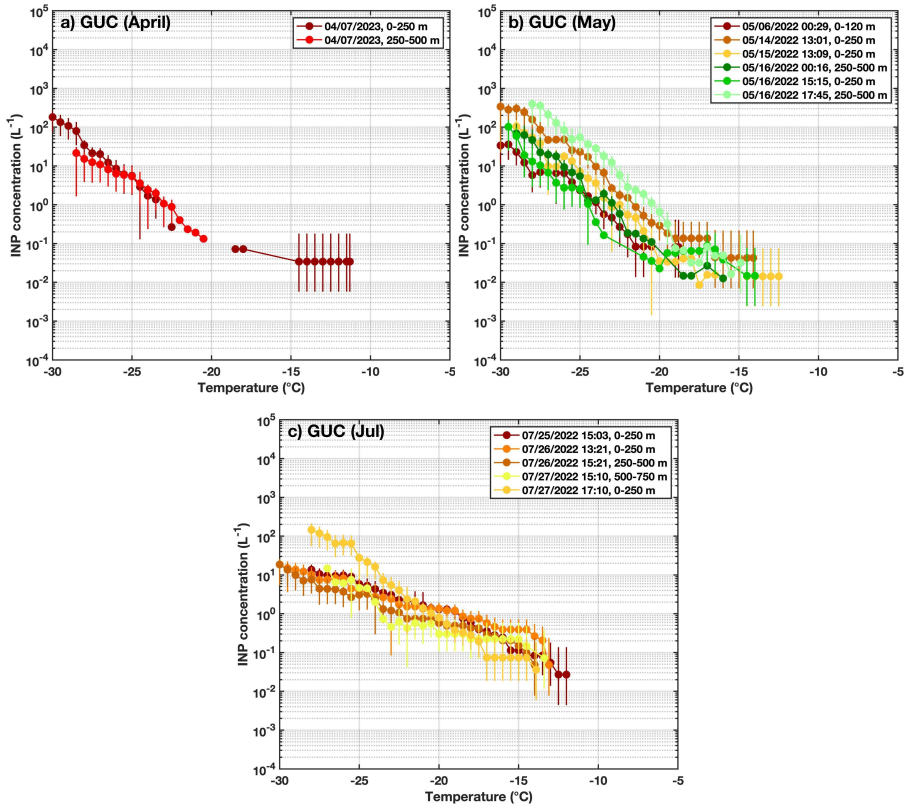

Figure S2. Same as Figure 5, but for GUC in a) April 2023, b) May 2022, and c) July 2022.

Deleted: 6

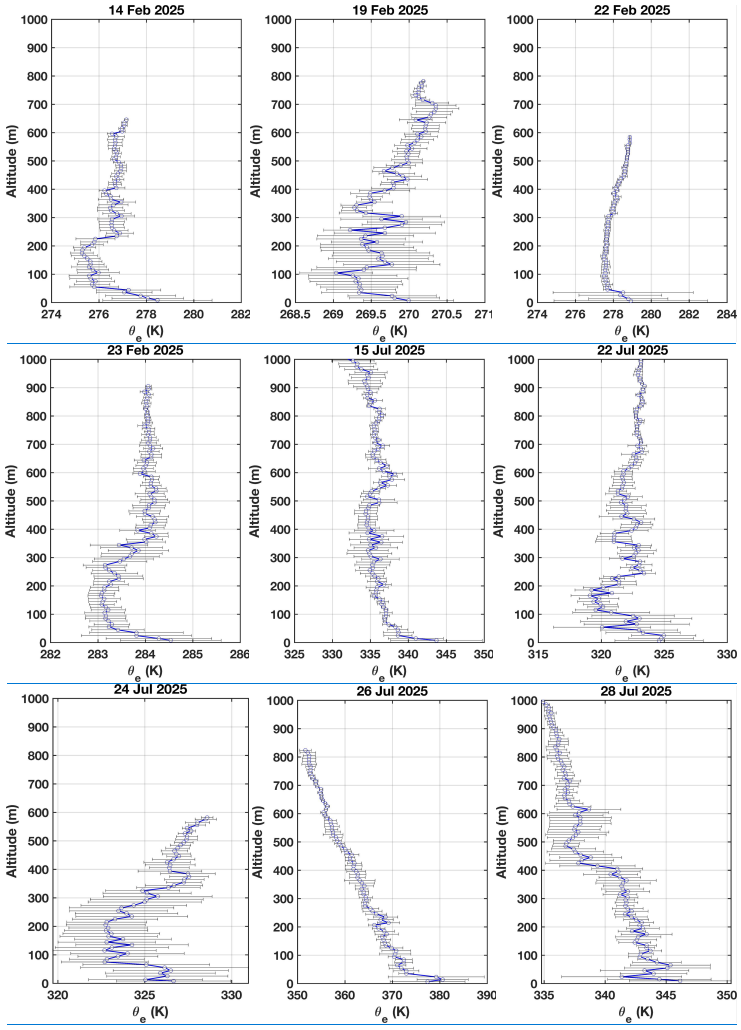

Figure S3. Vertical profiles of equivalent potential temperature (θ_e) in degrees K calculated based on Bolton (1980) from TBSIMET data from the CRG flights where PUFIN flew. Data are binned by every 10-m AMSL and focused on the lower 1000 m of the flight. Error bars represent one standard deviation.

Formatted: Font: Bold

Formatted: Subscript

Formatted: Justified, Space After: 0 pt

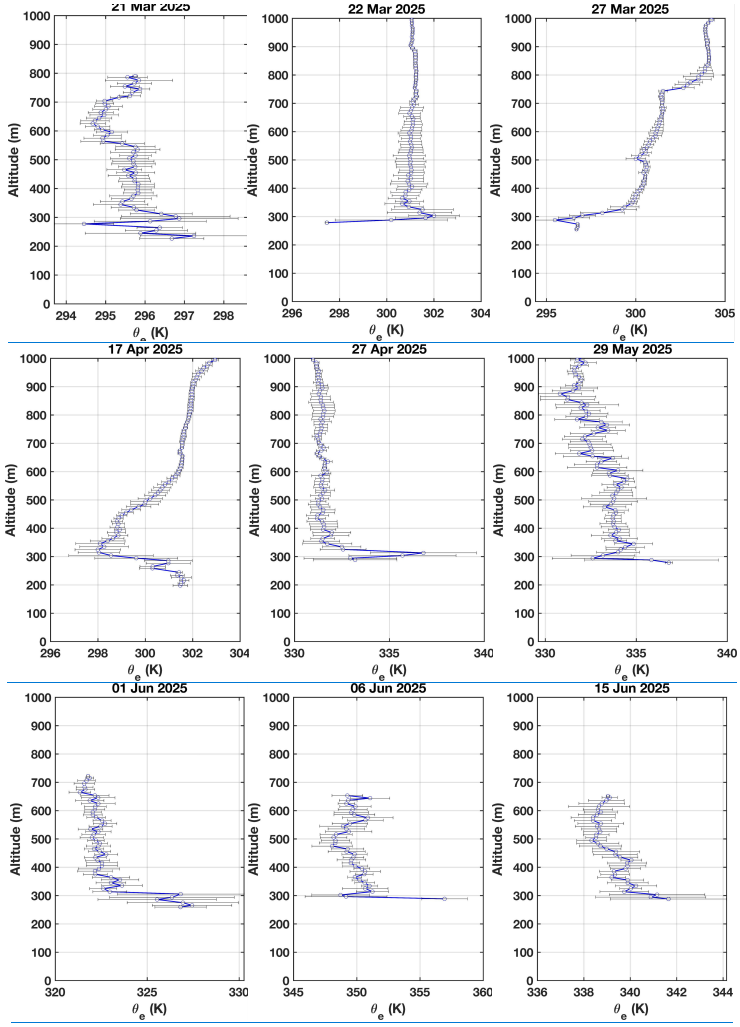

Figure S4. Same as Figure S3, but for BNF.

Formatted: Font: Bold

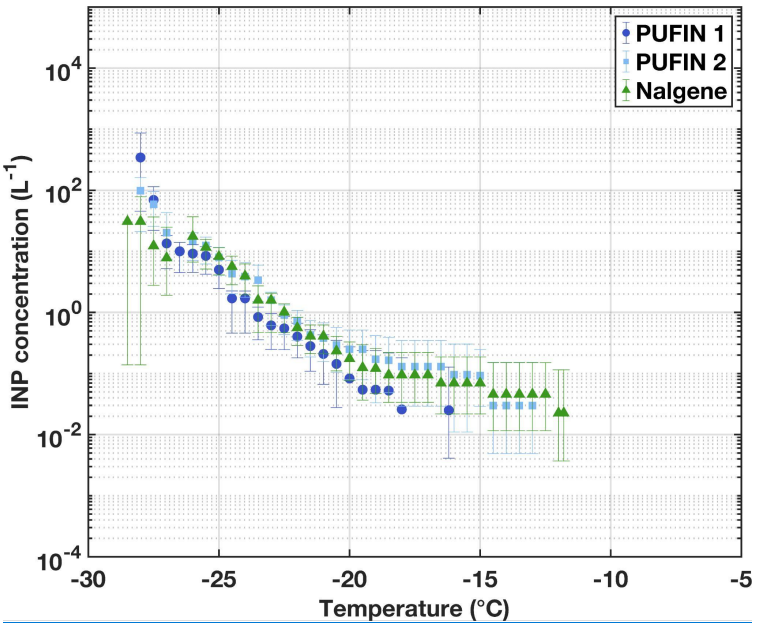

Figure S5. Cumulative INP spectra from both PUFIN units and the ARM ground-based Nalgene® filter unit (Creamean et al., 2025) for a 30-minute intercomparison test conducted outside the CSU building where the INS is housed.

Formatted: Font: Bold

Formatted: Superscript

Page 2: [1] Formatted	Jessie Creamean	4/12/26 3:58:00 PM

Font: Italic

Page 2: [1] Formatted	Jessie Creamean	4/12/26 3:58:00 PM

Font: Italic

Page 2: [1] Formatted	Jessie Creamean	4/12/26 3:58:00 PM

Font: Italic

Page 2: [1] Formatted	Jessie Creamean	4/12/26 3:58:00 PM

Font: Italic

Page 2: [1] Formatted	Jessie Creamean	4/12/26 3:58:00 PM

Font: Italic

Page 2: [1] Formatted	Jessie Creamean	4/12/26 3:58:00 PM

Font: Italic

Page 2: [1] Formatted	Jessie Creamean	4/12/26 3:58:00 PM

Font: Italic

Page 2: [1] Formatted	Jessie Creamean	4/12/26 3:58:00 PM

Font: Italic

Page 2: [1] Formatted	Jessie Creamean	4/12/26 3:58:00 PM

Font: Italic

Page 2: [1] Formatted	Jessie Creamean	4/12/26 3:58:00 PM

Font: Italic

Page 2: [1] Formatted	Jessie Creamean	4/12/26 3:58:00 PM

Font: Italic

Page 2: [1] Formatted	Jessie Creamean	4/12/26 3:58:00 PM

Font: Italic

Page 2: [1] Formatted	Jessie Creamean	4/12/26 3:58:00 PM

Font: Italic

Page 2: [1] Formatted	Jessie Creamean	4/12/26 3:58:00 PM

Font: Italic

Page 2: [1] Formatted **Jessie Creamean** **4/12/26 3:58:00 PM**

Font: Italic

Page 2: [1] Formatted **Jessie Creamean** **4/12/26 3:58:00 PM**

Font: Italic

Page 2: [1] Formatted **Jessie Creamean** **4/12/26 3:58:00 PM**

Font: Italic

Page 2: [1] Formatted **Jessie Creamean** **4/12/26 3:58:00 PM**

Font: Italic

Page 2: [1] Formatted **Jessie Creamean** **4/12/26 3:58:00 PM**

Font: Italic

Page 2: [1] Formatted **Jessie Creamean** **4/12/26 3:58:00 PM**

Font: Italic

Page 2: [1] Formatted **Jessie Creamean** **4/12/26 3:58:00 PM**

Font: Italic

Page 2: [1] Formatted **Jessie Creamean** **4/12/26 3:58:00 PM**

Font: Italic

Page 2: [1] Formatted **Jessie Creamean** **4/12/26 3:58:00 PM**

Font: Italic

Page 2: [1] Formatted **Jessie Creamean** **4/12/26 3:58:00 PM**

Font: Italic

Page 2: [1] Formatted **Jessie Creamean** **4/12/26 3:58:00 PM**

Font: Italic

Page 2: [1] Formatted **Jessie Creamean** **4/12/26 3:58:00 PM**

Font: Italic

Page 2: [1] Formatted **Jessie Creamean** **4/12/26 3:58:00 PM**

Font: Italic

Page 2: [1] Formatted **Jessie Creamean** **4/12/26 3:58:00 PM**

Font: Italic

Page 2: [1] Formatted	Jessie Creamean	4/12/26 3:58:00 PM

Font: Italic

Page 2: [1] Formatted	Jessie Creamean	4/12/26 3:58:00 PM

Font: Italic

Page 2: [1] Formatted	Jessie Creamean	4/12/26 3:58:00 PM

Font: Italic

Page 2: [1] Formatted	Jessie Creamean	4/12/26 3:58:00 PM

Font: Italic

Page 2: [1] Formatted	Jessie Creamean	4/12/26 3:58:00 PM

Font: Italic

Page 2: [1] Formatted	Jessie Creamean	4/12/26 3:58:00 PM

Font: Italic

Page 2: [1] Formatted	Jessie Creamean	4/12/26 3:58:00 PM

Font: Italic

Page 2: [1] Formatted	Jessie Creamean	4/12/26 3:58:00 PM

Font: Italic

Page 2: [1] Formatted	Jessie Creamean	4/12/26 3:58:00 PM

Font: Italic

Page 2: [1] Formatted	Jessie Creamean	4/12/26 3:58:00 PM

Font: Italic

Page 2: [1] Formatted	Jessie Creamean	4/12/26 3:58:00 PM

Font: Italic

Page 2: [1] Formatted	Jessie Creamean	4/12/26 3:58:00 PM

Font: Italic

Page 2: [1] Formatted	Jessie Creamean	4/12/26 3:58:00 PM

Font: Italic

Page 2: [1] Formatted	Jessie Creamean	4/12/26 3:58:00 PM

Font: Italic

Page 2: [1] Formatted	**Jessie Creamean**	**4/12/26 3:58:00 PM**

Font: Italic

Page 2: [1] Formatted	**Jessie Creamean**	**4/12/26 3:58:00 PM**

Font: Italic

Page 2: [1] Formatted	**Jessie Creamean**	**4/12/26 3:58:00 PM**

Font: Italic

Page 2: [2] Formatted	**Jessie Creamean**	**4/12/26 3:58:00 PM**

Font: Italic

Page 2: [2] Formatted	**Jessie Creamean**	**4/12/26 3:58:00 PM**

Font: Italic

Page 2: [2] Formatted	**Jessie Creamean**	**4/12/26 3:58:00 PM**

Font: Italic

Page 2: [2] Formatted	**Jessie Creamean**	**4/12/26 3:58:00 PM**

Font: Italic

Page 2: [2] Formatted	**Jessie Creamean**	**4/12/26 3:58:00 PM**

Font: Italic

Page 2: [2] Formatted	**Jessie Creamean**	**4/12/26 3:58:00 PM**

Font: Italic